International Journal of Energy and Environmental Engineering (2023) 14:573–599
https://doi.org/10.1007/s40095-022-00536-y

ORIGINAL RESEARCH

A state-of-the-art of experimentally studied adsorption water desalination systems

A. E. Zohir[1] · Ehab S. Ali[1] · A. M. Farid[1] · Ramadan N. Elshaer[1] · Ramy H. Mohammed[2] · Ahmed S. Alsaman[3] · Hamdy H. El-Ghetany[4] · Ahmed A. Askalany[3]

Received: 11 April 2022 / Accepted: 9 September 2022 / Published online: 23 September 2022

Abstract
Energy, freshwater, and the environment are interrelated features that infuse all human activities. Addressing this nexus in an integrated energy conversion system is a big challenge for the research community. Adsorption desalination system, which is a good alternative to traditional desalination systems, could solve this problem because it uses eco-friendly working fluids and can be powered by renewable energy. Many experimental prototypes for the adsorption desalination cycle were built and tested in the last decades. Also, different adsorbent materials were developed and characterized. Therefore, this paper reviews adsorbent materials with water vapor utilized in experimental adsorption desalination studies, which is considered the first step in constructing an efficient system. After that, the paper comprehensively reviews all previous experimental adsorption desalination studies. It focuses on the design of the experimental test rig, the mass of adsorbent material, and system performance, such as the specific daily water production, coefficient of performance, and specific cooling power. This work also discusses the properties of heat exchangers (i.e., adsorbent beds) employed in adsorption desalination systems.

Keywords Adsorption cycles · Adsorbents · Desalination · Energy-efficient

Introduction

Energy, freshwater, and the environment are interrelated features that infuse all our activities on the earth. Furthermore, they are becoming the most significant and common areas in recent research fields [1]. World energy consumption is projected to increase by 2.6% annually to 2030 [2]. The electrical energy utilization growth rate in Egypt is about 7% annually. It would need to increase its current generation capacity by a higher rate (more than 7%). The energy rate utilized by refrigeration air conditioning systems represents 30% of the total worldwide consumed energy and 32% in Egypt [3].

Due to population growth, desalination is a practical solution to the water shortage problem [4]. Distillation, membrane, and crystallization are examples of traditional desalination methods. Membrane-based reverse osmosis (RO), multi-stage flashing (MSF), and multi-effect distillation (MED) are examples of commercial desalination technologies [5]. Table 1 expresses comparing analysis for almost all common desalination technologies [6]. On the other hand, traditional desalination technologies have a significant initial investment and running cost [7, 8]. The energy costs of producing unit water by MSF or RO are higher than producing potable water from surface and subterranean water resources. Desalination costs vary depending on the location. The cheapest seawater reverse osmosis cost was 0.5 US$/m^3 in 2016 [9]. Traditional energy-based desalination plants consume a lot of natural resources. As a result, solar, geothermal, wind, and other pollutant-free renewable energy sources are becoming increasingly popular for desalination. However, more research is needed to identify the most suitable technology for desalination applications [10].

✉ Ehab S. Ali
eng_ehab1987@yahoo.com

1 Mechanical Engineering Department, Tabbin Institute for Metallurgical Studies, Cairo 11912, Egypt

2 Department of Mechanical Power Engineering, Zagazig University, Zagazig 44519, Egypt

3 Mechanical Department, Faculty of Technology and Education, Sohag University, Sohag 82524, Egypt

4 Solar Energy Department, National Research Centre, Cairo 12622, Egypt

Table 1 Comparing analysis for almost common desalination technologies [6]

Items	MSF	MED	MED-TVC	SWRO	MD	(MED + AD)
Driving temperature (°C)	90–110	65–70	65–70	Ambient	60–90	65–70
Capital cost ($/m^3/day)	1598	2000	1860	1313	1131	2200
Thermal energy (kWh$_{thermal}$/m^3)	53–70	40–65	50–80	–	100	30–40
Electrical energy (kWh$_{elec}$/m^3)	2.5–5.0	2.0–2.5	2.0–2.5	4.0–6.0	1.5–3.65	2.8
Water cost ($/m^3)	0.56–1.75	0.52–1.01	1.12–1.50	0.26–0.54	1.17–2.0	0.48

Adsorption desalination system (ADS) is becoming a promising future technology for saving the required freshwater [11, 12]. It is based on using porous material that could be regenerated via low-grade thermal energy [13, 14]. The ADS has the advantage of efficiently utilizing low heat sources such as waste heat and/or solar energy [15–17]. It has some advantages over the commercial desalination methods, such as (i) the employment of the low-temperature excess or waste heat, (ii) lesser corrosion and fouling, (iii) and low maintenance cost. In addition, the ADS has two significant outcomes over the current desalination technologies, namely, (i) removing any "bio-contamination" and (ii) decreasing global warming due to the employment of excess waste heat [2, 18, 19]. The adsorption system can also be driven by renewable energy, reducing global warming resulting from carbon dioxide emissions of electricity generation [20]. The adsorption systems can be utilized for cooling purposes [21, 22]. The idea for utilizing these systems in desalination was firstly presented by Zejli et al. [23] in 2004, in which the earliest ADS simulation was performed. Till now, mathematical results [4–6, 24–28] achieved high values of specific daily water production (SDWP) and coefficient of performance (COP) of 98 m^3/ton.day and 2.1, respectively [4]. However, this performance was not proven experimentally on either lab-scale, prototype, or pilot scale. Experimental measurements are still low as SDWP did not increase more than 18 m^3/ton.day [29], and COP did not increase than 0.77 [30]. This trend shows a research gap between the theoretical and experimental studies in this field because of the lack of understanding of the effect of heat and mass transfer mechanisms on cycle performance. Also, many adsorbent materials have been developed in the last years, and however, their performance was tested theoretically without considerable investigation about their thermal effect on the system performance [14, 31].

Therefore, the present review presents an innovative review focusing on experimental studies of ADS. It also discusses the effect of the employed adsorbents' heat and mass transfer characteristics on the system efficiency for the first time in reviewing ADS. Thus, the paper identifies the huge difference in performance between the experimental and numerical studies in adsorption desalination. It also discusses this technology's future perspective, challenges, and outlook to fill the world water demand and supply gap. The present review is divided into two main sections besides the introduction. The first section explores research that expresses experimental adsorbent materials with water vapor, which is the first step in constructing an ADS. The second section explores experimental investigations for ADS with and without evaporator condenser heat recovery. This work emphasizes the experimental test rig design, the mass of adsorbent material adsorption, and desalination system performance as SDWP, COP, and specific cooling power (SCP) for each experimental device. This review states the properties of utilized heat exchangers of adsorbent beds in ADS.

Adsorbent materials used in ADS

Many researchers focused on developing new adsorbent material or improving its adsorption uptake to enhance ADS effectiveness. Therefore, this section presents adsorption materials tested with water vapor as adsorbate.

Silica gel

Silica gel is the common material utilized in the ADS. Silica gel is a category of amorphous synthetic silica that consists of a rigid and continuous net of colloidal silica associated with SiO_4 particles. The main advantages of silica gel are that it can regenerate with temperatures as low as 100 °C and thermal stability. Still, they have low adsorption capacity compared to new adsorbents such as MOF [15]. White [32] theoretically illustrated the effect of silica gel granular diameter (1, 2, 3 mm) on the water adsorption rate. The study showed that reducing granule size raises the adsorption rate. Table 2 summarizes different types of silica gel and their adsorption uptakes.

Zeolite

Zeolite is a crystalline alumina silicate composed of alkali/alkali soil, namely molecular sieve, and alumina silicate skeletal has 0.2–0.5 cm^3/g of porosity. The adsorption capability of zeolite is related to the proportion between aluminum and silicon. The main advantages of zeolite are non-toxic, non-flammable, and environmentally friendly. It

Table 2 Different types of silica gel and their adsorption uptakes

Silica gel	Max. equilibrium uptake (gwater g^{-1}_{ads})	BET surface area (m^2 g^{-1})	References
Silica gel, type 3A/H_2O	0.33	n.d	[33]
Silica gel, type A/H_2O	0.40	n.d	[33]
Silica gel, type A + +/H_2O	0.52	863.6	[33]
Silica gel, type 2560/H_2O	0.32	636.4	[33]
Silica gel, type RD/H_2O	0.45	838	[34]
Fuji silica gel, type RD/H_2O	0.48	780	[35]
Fuji silica gel, type 2060/H_2O	0.37	707	[35]

n.d. means no data

Table 3 Different types of zeolite and their adsorption uptakes

Zeolite	Max. equilibrium uptake (gwater g^{-1}_{ads})	BET surface area (m^2 g^{-1})	References
Natural zeolite/H_2O	0.12	643	[38]
Zeolite 4A/H_2O	0.20	n.d	[38]
AQSOA-Z01/H_2O	0.21	189.6	[39]
AQSOA-Z02/H_2O	0.31	717.8	[39]
AQSOA-Z05/H_2O	0.23	187.1	[39]
Zeolite-13X/H_2O	0.30	n.d	[40]

n.d. means no data

needs high regeneration temperatures and low adsorption capacity compared to new adsorbents such as MOF [36]. About 40 types of natural zeolite and around 150 types of artificial zeolite regarding a synthesis method [37]. Table 3 summarizes different types of zeolite and their adsorption uptakes.

Metal–organic frameworks (MOFs)

Heat transformation technologies require the creation of adsorbent materials. In this regard, new materials appropriate to adsorption–desorption working fluid must yet be discovered for this technology to be remarkable [41, 42]. Metal–organic frameworks (MOFs), also known as porous coordination polymers (PCPs), have shown outstanding adsorbent properties and were investigated for heat transformation uses. MOFs also comprise hydrophilic and hydrophobic moieties, each with adsorption characteristics. Because of their high adsorption capacity for guest molecules such as water, MOF materials offer significant potential for heat transformation compared to a large range of natural and manufactured adsorbents. However, their stability and long-time synthesis process are the main challenges facing this family of nanoporous materials [42, 43]. Compared to silica gel, MOFs with hydrophilic characteristics have the preference since they have an unlimited water uptake capacity at high pressures. At first, MOFs were demonstrated as adsorbent materials by looking at their ability to use solid–gas adsorption for energy transformations. MOF materials offer a wide range of energy storage and heat transformation (cooling/heating) uses. Because water is commonly utilized as a working fluid, the examined adsorbent materials were evaluated using water adsorption–desorption properties. MOFs have also been examined for water adsorption studies to investigate structural characteristics and adsorption performance. The metal clusters must first coordinate water molecules before the poetical condensation procedure in the solid adsorbent's pores (MOFs) occurs in water adsorption [42, 44]. Therefore, metal groups categorize MOF materials for water adsorption and heat/energy transformation applications. In addition, several frameworks showed geometric plasticity and reversible structural change in guest adsorption. Thus, water adsorption on MOF materials was previously used to estimate their heat transformation performance.

MOFs have significantly more promise for this use than current adsorbents for heat transformation applications, like alumina phosphates or zeolites, owing to their composition, pore structure, also topology. Furthermore, additional improvement of the porosity structure of the MOFs, allowing for tailoring of their adsorption capabilities, modification or functionalization of metal clusters/ions, and biological linkers are still achievable [42, 45]. This opens up exciting possibilities for MOF production with specified properties optimized for specific working situations, such as heat transformations [42, 43]. Interestingly, development in MOF chemistry has progressed. Numerous techniques to synthesize and develop water-stable MOFs have paved the path for water-sorbent candidates with improved water adsorption and associated applications, see Table 4 [46–50]. From where water uptake capacity and corresponding relative pressure at which the pore filling occurs, the adsorption capabilities of MOFs are highly variable from a qualitative standpoint. Hydrolytically stable porous materials with large pore volumes, on the other hand, are likely to have large water adsorption capabilities. Hunt for hydrolytically stable

Table 4 List of possible MOFs and their water adsorption properties

MOFs	Metals	Uptake[a] (gwater g^{-1}ads)	Surface area (m^2 g^{-1})	References
CAU-6	Al	0.485	620	[54]
CAU-10	Al	0.31	635	[55]
CAU-10-H	Al	0.382	635	[55]
CAU-10-NH_2	Al	0.19	n.d	[55]
CAU-10-NO_2	Al	0.15	440	[55]
CAU-10-OCH_3	Al	0.07	n.d	[55]
CAU-10-OH	Al	0.27	n.d	[55]
DUT-4	Al	0.28	1360	[44]
DUT-67	Zr	0.625	1560	[56]
MIL-100	Cr	0.41	1517	[57]
MIL-100	Fe	0.81	1549	[44]
		0.77	1917	[58]
MIL-100	Al	0.50	1814	[58]
MIL-100	Cr	0.40	1330	[59]
		1.01	2059	[60]
		1.28	3017	[44]
		1.40	3124	[61]
MIL-100-DEG	Cr	0.33	580	[59]
MIL-100-EG	Cr	0.43	710	[59]
MIL-101-NH_2	Cr	0.90	2509	[61]
		1.06	2690	[62]
MIL-101-NO_2	Cr	1.08	2146	[61]
		0.44	1245	[62]
MIL-101-pNH_2	Cr	1.05	2495	[62]
MIL-101-pNO_2	Cr	0.60	2195	[62]
MIL-101-soc	Cr	1.95	4549	[53]
MIL-125	Ti	0.36	1160	[45]
MIL-125-NH_2	Ti	0.36	830	[45]
		0.37	1220	[63]
MIL-53	Al	0.09	1040	[45]
		0.09	n.d	[64]
MIL-53-NH_2	Al	0.05	940	[45]
		0.09	n.d	[64]
MIL-53-OH	Al	0.40	n.d	[64]
MIL-53	Ga	0.05	1230	[45]
MIL-53-NH_2	Ga	0.02	210	[45]
MIL-53-$(COOH)_2$	Fe	0.16	n.d	[64]
MIL-68	In	0.32	1100	[45]
MIL-68-NH_2	In	0.32	850	[45]
MOF(NDI-SEt)	Zn	0.25	888	[65]
MOF(NDI-SO2Et)	Zn	0.25	764	[65]
MOF(NDI-SOEt)	Zn	0.30	927	[65]
MOF-199	Cu	0.55	1340	[44]
		0.64	921	[66]
		0.49	1270	[67]
MOF-74	Co	0.63	1130	[56]
MOF-74	Mg	0.75	1250	[56]
		0.62	1400	[67]
MOF-74	Ni	0.615	1040	[56]
		0.48	639	[56]
MOF-801-P	Zr	0.45	990	[56]
MOF-801-SC	Zr	0.35	690	[56]
MOF-802	Zr	0.11	1290	[56]
MOF-804	Zr	0.29	1145	[56]
MOF-805	Zr	0.415	1230	[56]
MOF-806	Zr	0.425	2220	[56]
MOF-808	Zr	0.735	2060	[56]
MOF-841	Zr	0.64	1390	[56]
PIZOF-2	Zr	0.85	2080	[56]
SIM-1	Zn	0.14	570	[45]
UiO-60	Zr	0.535	1290	[56]
		0.40	1032	[63]
		0.39	1105	[68]
		0.37	1160	[67]
UiO-66–1,4-Naphy1	Zr	0.26	757	[68]
UiO-66–2.5-$(OMe)_2$	Zr	0.42	868	[68]
UiO-66-NH_2	Zr	0.38	1328	[63]
		0.34	1123	[68]
		0.37	1040	[67]
UiO-66-NO_2	Zr	0.37	792	[68]
UiO-67	Zr	0.18	2064	[63]
ZIF-8	Zn	0.02	1255	[44]
		0.01	1530	[45]

[a]Adsorption properties of water measured at 25 °C and almost saturated vapor pressure

and recyclable MOFs with higher total water uptake is a major focus of MOF chemistry research [45, 47, 51–53].

Comparison among MOF materials and conventional materials

The authors showed and compared various MOF materials that outperform existing porous materials like silica gel and zeolites in water adsorption [69, 70], see Fig. 1. The water adsorption isotherms of MOF materials are shown in Fig. 2. When comparing Figs. 1 and 2, it is clear that the MIL-101(Cr) outperformed the typical greatest adsorption capacity. For the adsorption (desalination and cooling) process, desalinated water and cooling effects are influenced by the value of the adsorption capacity of the adsorbent material. The available adsorbed amount in water vapor adsorption uptake (Δw) at adsorption and adsorption pressures are mainly affected by the available adsorbed amount. The Δw represents the difference between expected material concentrations in the adsorption and desorption model

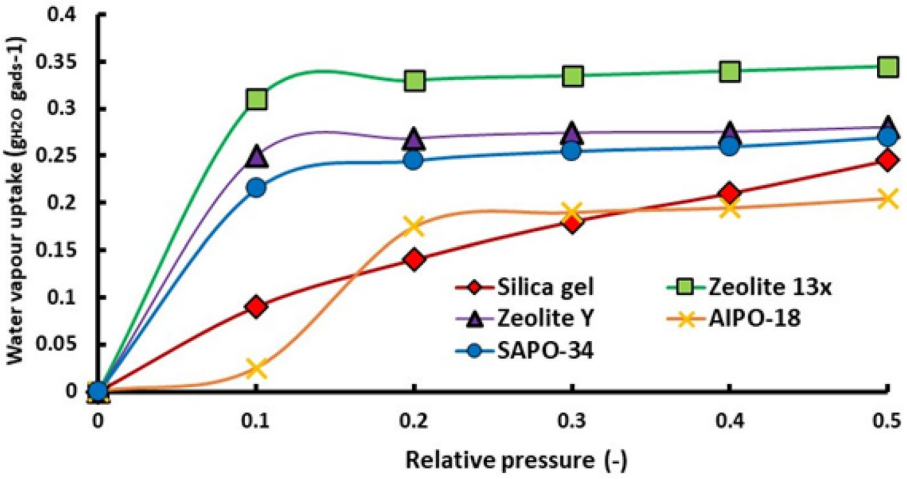

Fig. 1 Isotherms for water adsorption of traditional adsorbents like silica gel RD [75], SAPO-34 [72], Zeolite Y [76], Zeolite 13X [77]and AlPO-18 [77] at 25 °C

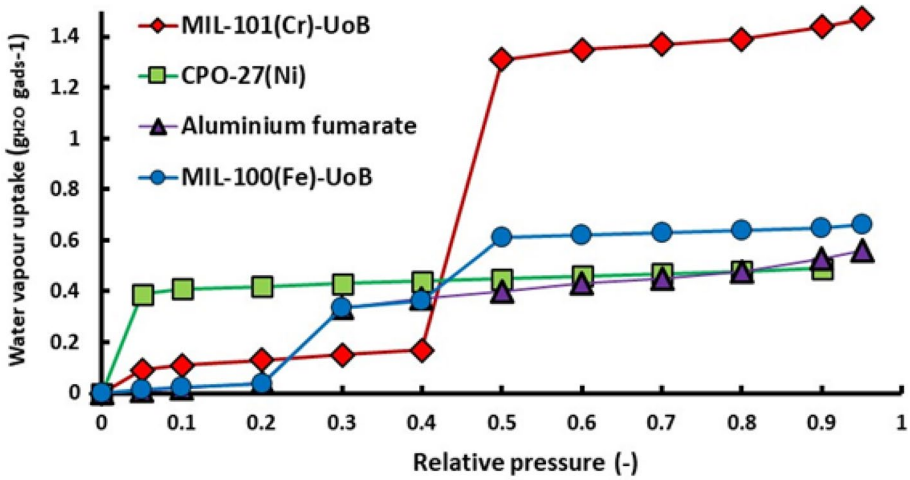

Fig. 2 Isotherm of water adsorption for some MOF materials like MIL-101(Cr)-UoB, CPO-27(Ni), Aluminum fumarate, and MiL-100(Fe)-UoB [69] at 25 °C

(cycle sorption quantity). The adsorbent material with a step increase in water vapor uptake before ($P/P_s = 0.25$) is suitable for cooling applications. Some adsorbent materials take their most adsorption capacity after $P/P_s = 50\%$, which indicates that it is more suitable for desalination than cooling applications. In cooling applications, the evaporator pressure could be considered 1 kPa to get a cooling effect at around 7 °C, while in the desalination application, the evaporator pressure could be higher, around 2.25 kPa to take benefit most adsorption capacity of material as Δw [36]. Based on this Figure, MIL-101(Cr), MIL-100(Fe), and aluminum fumarate are suitable for applications requiring high P/P_s, like desalination [68] or energy storage, whereas CPO-27(Ni) is better suited for applications requiring low P/P_s like energy storage [71], cooling [72] or dual effect desalination [73, 74]. For more illustration of whether an adsorbent is suitable more in desalination or cooling applications, or both. This is calculated based on Δw at evaporation and condensation pressures and temperatures using the Gibbs energy change ($-\mathrm{RT}\ \ln(P/P_s)$) relationship as illustrated in Fig. 3. The figure expresses that the MIL-101(Cr)-UoB has the best performance in desalination mode. It is achieved Δw (1.22 kg/kg) in desalination application. But it has not a good performance in cooling mode as it achieves Δw (0.06 kg/kg) due to its isotherm performance, which has a jump in adsorbed vapor uptake after $P/P_s = 0.4$. The figure also expresses that Aluminum fumarate and MIL-100(Fe)-UoB have the best performance in cooling mode as they achieve around Δw (0.32 kg/kg) in cooling mode.

Enhancing the properties of MOF materials

Because of its huge pore size and high free volume, MIL-101(Cr) has exceptional features, including exceptionally low thermal conductivity. During both adsorption and desorption stages, low thermal conductivity makes it difficult for heat transfer processes to reach the required operating temperatures fast. To enhance the thermal conductivity of parent MIL-101, a composite of MIL-101(Cr)/GrO was utilized (Cr) [78]. Two approaches were used to create a composite of MIL-101(Cr)

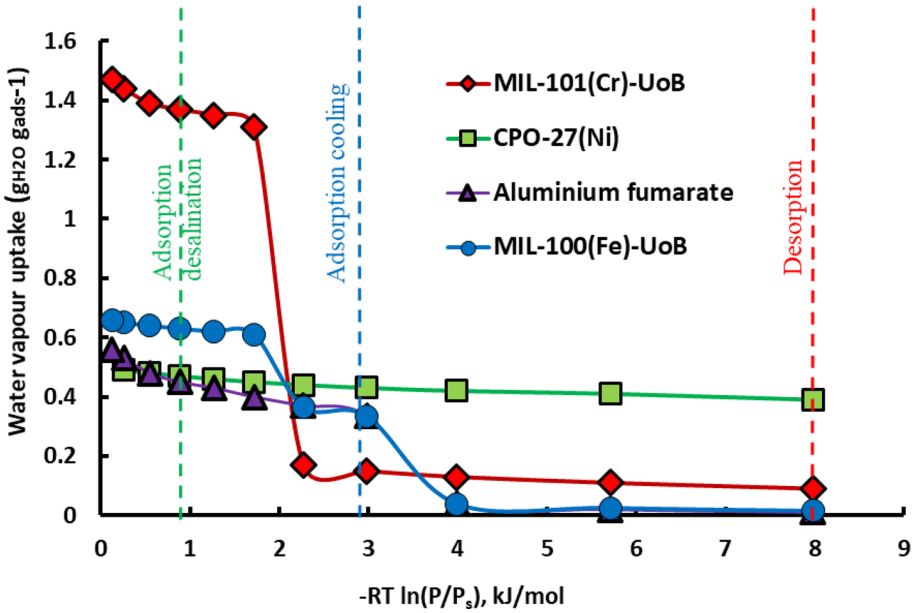

Fig. 3 Adsorption characteristic of MOF [69] at 25 °C

and GrO: physically mixing the two components and integrating them into the synthesis process. Owing to the limited porosity of GrO, it was discovered that the composites made via the physical mixing method had a decreased water uptake. In the synthesis process, the 2% GrO synthesis composite demonstrated comparable water uptake at low relative pressures and outperformed the pristine material at high relative pressures. Because of the crystal structural distortion, 5% GrO synthesis composite reduced water uptake [78].

Composite adsorption materials

Many researchers have improved the current adsorbent materials by the composition method, whether by compositing two or more host matrix materials together or by compositing a host matrix with a salt hydrate to improve the performance of systems that use those materials [36]. Table 5 summarizes the adsorption characteristics of composite materials. The table illustrates that composite adsorbent materials achieved higher adsorption water capacity than the base materials, which expresses that composite materials can achieve higher performance as cooling power or desalination effect. But these composite adsorbents need to be examined experimentally in adsorption desalination/cooling devices to realize what can enhance performance.

Experimental adsorption desalination systems

This section explores all presented experimental investigations for ADS separated into two categories. Experimental investigation types are ADS with and without evaporator condenser heat recovery. This section explores all experimental adsorption desalination (AD) studies; the work emphasizes the experimental test rig design, the mass of adsorbent material adsorption, and desalination system performance as SDWP, COP, and specific cooling power (SCP) of each experimental device. This work also reviews the properties of the used heat exchangers of adsorbent beds in ADS.

Experimental adsorption desalination studies

In this sub-section, experimental investigations of ADS are presented. These experimental investigations are for producing both desalination and cooling effects. The first excremental test rig for ADS was presented by Wang et al. [8], as illustrated in Fig. 4. The highest SDWP obtained was 4.7 m^3/ton of silica gel at T_{des} = 85 °C and T_{cw} = 30 °C. This study also reported that SDWP yielded from the plant could be further boosted by adopting a higher chilled water temperature supply (T_{chi}) and lowering adsorption cooling water (T_{cwi}). It demonstrated that ADS was also more efficient when the heat source temperature was lowered to 65 °C. Thu et al. [118] reported ADS performances with two-bed and four-bed operational modes. Figure 5 shows the used test rig for ADS. The tested results are estimated in terms of (i) SDWP, cycle time, and (ii) performance ratio (PR) for several driving temperatures (T_{drv}). It was found that the maximum SDWP is about 10 m^3 /tone.day with PR 0.61. The study also provided a valuable guideline for the operational approach of ADS. The study employed four adsorption units with 36 kg of silica gel per adsorption unit. Wu et al. [119] presented ADS as an alternative to traditional desalination systems that could be utilized by waste heat

Table 5 Summary of the adsorption characteristics of composite materials

Composite	Uptake (g g^{-1})	BET surface area (m^2 g^{-1})	V_{por} (cm^3 g^{-1})	P/P_s (–)	T_{ads} (°C)	Refs.
SG/$CaCl_2$	1			> 0.6	20	[79]
SG	0.4	785	1.31	0.95	23	[80]
SG/$CaCl_2$	0.57	224	1.039			
SG/16.7wt.% $CaCl_2$	0.57	886	3.9	0.75	25	[81]
SG/28.9wt.% $CaCl_2$	0.9	640	1.9	0.75		
SG/16.6wt.% $CaCl_2$	0.48	276	0.45	0.75		
SG/28.9wt.% $CaCl_2$	1.1	200	0.54	0.75		
SG/31.6wt.% $CaCl_2$	0.68	152	0.54	0.7		
SG	0.16	529	0.806	0.8	30	[82]
SG/10wt.% $CaCl_2$	0.44		0.698			
SG/20wt.% $CaCl_2$	0.53		0.567			
SG/30wt.% $CaCl_2$	0.6		0.53			
SG/40wt.% $CaCl_2$	0.74		0.395			
SG	0.1	550	0.43	0.75		[83]
SG/28.6wt.% LiBr (Aerogel)	0.5	520	1.05	0.7	25	
SG/28.6wt.% LiBr (Densified)	0.68	351	1.13	0.75		
SG/28.0wt.% LiBr (Xerogel)	0.63	324	0.38	0.75		
SG/35.5wt.% LiBr (Impregnation)	0.8	262	0.39	0.65		
SG/13.5wt.% $MgSO_4$	0.27				25	[84]
SG/24wt.% $MgSO_4$	0.37					
SG/38wt.% $MgSO_4$	0.47					
KSM SG		600	0.3			[85]
KSM SG/21.7 wt.% $CaCl_2$	0.25			0.7	20	
KSK SG		260	1			[86]
KSK SG/45wt.% $Ca(NO_3)_2$	0.2–0.3	60	0.24	< 0.7	30	
KSK SG		350	1		35	[87]
KSK SG/34.5wt.% $LiNO_3$	0.22					
KSK SG			1		20	[88]
KSK SG/42wt.% $CaCl_2$	0.45		0.6–0.64			
KSK SG/48wt.% LiBr-	0.39		0.6–0.64			
KSK SG/33wt.% $MgCl_2$	0.51		0.6–0.64			
KSKG SG		350	1			[89]
KSKG SG/33.7 wt.% $CaCl_2$	0.7–0.75			0.7	20	
KSKG SG/32 wt.% LiBr	0.6–1			0.7–0.8	40	[90]
KSKG SG/57 wt.% LiBr						
PHTS	0.16–0.65	810	0.705	0.4–0.95	40	[91]
PHTS/4wt.% $CaCl_2$	0.25–0.78	461	0.492			
PHTS/10wt.% $CaCl_2$	0.38–1.20	322	0.377			
PHTS/20wt.% $CaCl_2$	0.58–2.24	163	0.189			
SBA-15		519	0.73		50	[92]
SBA-15/43wt.% $CaCl_2$	0.615	52	0.17	0.4		
SBA-15	0.02	554	0.8	0.3	20	[93]
SBA-15/2.80wt.% $Al_2(SO_4)_3$	0.05	550	0.75			
SBA-15/5.32wt.% $Al_2(SO_4)_3$	0.065	549	0.73			
SBA-15/6.77wt.% $Al_2(SO_4)_3$	0.09	541	0.7			
Syloid72FP/Emim-Oms	1.64			0.9	25	[94]
Syloid AL-1FP	0.28	605–740	0.23–0.4	0.9	25	[95]
Syloid AL-1FP/60wt.% Emim-Oms	1.86					
Syloid AL-1FP/20wt.% Emim-Ac	0.92					

Table 5 (continued)

Composite	Uptake (g g^{-1})	BET surface area (m^2 g^{-1})	V_{por} (cm^3 g^{-1})	P/P_s (–)	T_{ads} (°C)	Refs.
Syloid72FP	0.44	340–405	1.2			
Syloid72FP/60wt.% Emim-Oms	1					
Syloid72FP/60wt.% Emim-Ac	1.32					
Syloid AL-1FP/60.0% [Emim][CH_3SO_3]	0.85			0.9	25	[96]
Syloid AL-1FP/41.7% [Emim][CH_3SO_3]	0.75					
Syloid AL-1FP/17% [Emim][CH_3SO_3]	0.5					
Syloid AL-1FP/1.8% [Emim][CH_3SO_3]	0.25					
AC	0.35	678	2.365	0.94	23	[97]
AC/$CaCl_2$	0.42	224	1.039			
AC/38.6wt.% $MgCl_2$	0.941	716	0.3924	0.7	25	[98]
AC/31.2wt.% MgCl2 + 3.2wt.% Ce	1.05	494.8	0.3846			
AC	0.19	1117	0.5329	atm	25	[99]
AC + 16wt.%SG	0.244	610	0.2934			
AC + 26wt.%SG	0.246	664	0.3121			
AC + 19wt.%SG	0.25	682	0.3242			
AC + 2wt.%SG/68wt.%$CaCl_2$	0.41	118	0.074			
AC + 4wt.%SG/57wt.%$CaCl_2$	0.699	82	0.0449			
AC + 3wt.%SG/64wt.%$CaCl_2$	0.805	83	0.0589			
AC + 20wt.%SG/11wt.%$CaCl_2$	0.243	602	0.2895			
AC + 24wt.%SG/13wt.%$CaCl_2$	0.236	626	0.2975			
AC + 22wt.%SG/4wt.%$CaCl_2$	0.264	680	0.327			
AC + 22wt.%SG/5wt.%$CaCl_2$	0.412	156	0.0812			
AC + 13wt.%SG/21wt.%$CaCl_2$	0.433	160	0.0882			
AC + 10wt.%SG/15wt.%$CaCl_2$	0.332	188	0.0958			
AC1		1370	0.109	0.4–0.9		[100]
AC1/10wt.% Na_2O_3Si	0.12–0.52	690	0.095		25	
AC2		1300	0.158			
AC2/10wt.% Na_2O_3Si	0.12–0.42	1080	0.048			
Carbon Sibunit		450 ± 25	0.9 ± 0.05			[97]
Carbon Sibunit/29wt.% LiBr	0.4–1.1			0.7	30	
Expanded graphite		12.3 ± 1.2	3.3 ± 0.1			
Expanded graphite/33wt.% LiBr	0.4–1.1			0.7	30	
MWCNT		270	3	> 0.4	37	[101]
MWCNT/44wt.% LiCl	1.1	140	1.4			
MWCNT/53wt.% $CaCl_2$	0.94	75	0.9			
MWCNT		270	5.3		35	[102]
GP(MWCNT/41wt.% LiCl)	1	145	2.7			
PB(MWCNT/42wt.% LiCl)	1	124	4.7			
PP(MWCNT/41wt.% LiCl)	1	144	2.7			
MWCNT/PVA/55wt.% LiCL	0.6	80	0.9	0.2	35	[103]
Zeolite		921	0.374			[104]
Zeolite/15wt.% $MgSO_4$	0.15	400	0.18	0.7	30	
Zeolite13X	0.28	468	1.527	0.94	23	[80]
Zeolite13X/$CaCl_2$	0.6	233	1.489			
Zeolite13X	0.0761	667	0.32	< 0.3	25	[105]
Zeolite13X/10wt.% $CaCl_2$	0.0914	608	0.34			
Zeolite13X/20wt.% $CaCl_2$	0.1592	608	0.36			
Zeolite13X/30wt.% $CaCl_2$	0.1953	605	0.36			
Zeolite13X/40wt.% $CaCl_2$	0.3953	601	0.34			

Table 5 (continued)

Composite	Uptake (g g^{-1})	BET surface area (m^2 g^{-1})	V_{por} (cm^3 g^{-1})	P/P_s (–)	T_{ads} (°C)	Refs.
Zeolite13X/46wt.% $CaCl_2$	0.8	622	0.54			
Alumina/Zeolite13X	1.16	455	0.283	0.94	20	[106]
Alumina			0.75		20	[92]
IK-02-200 alumina/31wt.% $CaCl_2$	0.3		0.6–0.64			
MIL-101	0.18	3402.69	1.59	0.4	25	[107]
MIL-101/LiCl	0.5	2054.03	0.94			
MIL-101/NaCl	0.46	2000.66	0.91			
MIL-101	1.22	2789	1.32	0.9	25	[108]
MIL-101/2wt.% GO	1.53	3472	1.69			
MIL-101/4wt.% GO	1.56	3501	1.77			
MIL-101/6wt.% GO	1.58	3522	1.78			
MIL-101/8wt.% GO	1.42	3126	1.57			
MIL-101(Cr)	0.1–1.35	3354.84	1.73	0.3–0.9	25	[109]
MIL-101(Cr)/3wt.% $CaCl_2$	0.16–1.2	2976.77	1.49			
MIL-101(Cr)/4wt.% $CaCl_2$	0.16–1.3	3117.14	1.58			
MIL-101(Cr)/5wt.% $CaCl_2$	0.26–1.2	2675.9	1.35			
MIL-101(Cr)/6wt.% $CaCl_2$	0.22–1.25	2641.5	1.32			
MIL-101(Cr)/8wt.% $CaCl_2$	0.65–1.75	1876.01	0.99			
MIL-101(Cr)	0.18–1.05	2824	1.362	0.4–0.9	25	[110]
MIL-101(Cr)/10% $CaCl_2$	0.5–0.88	1977	0.745			
MIL-101(Cr)/20% $CaCl_2$	0.53–1.13	1307	0.509			
MIL-101(Cr)/30% $CaCl_2$	0.6–1.35	193	0.071			
MIL-101(Cr)	0.4	3460	1.753	0.95	25	[78]
MIL-101(Cr)/0.5wt.%GrO (Synthesis)	1.4	3137.8	1.641			
MIL-101(Cr)/0.5wt.%GrO (Physical)	1.22	2608.5	1.346			
MIL-101(Cr)/1wt.%GrO (Synthesis)	1.45	3028.1	1.619			
MIL-101(Cr)/1wt.%GrO (Physical)	1.17	2425.7	1.265			
MIL-101(Cr)/2wt.%GrO (Synthesis)	1.55	3674	2.14			
MIL-101(Cr)/2wt.%GrO (Physical)	1.32	2077	1.035			
MIL-101(Cr)/5wt.%GrO (Synthesis)	1.47	2810	1.879			
MIL-101(Cr)/5wt.%GrO (Physical)	1.27	2626	1.33			
Vermiculite	0.06	15.1	4.11	0.94	23	[80]
Vermiculite/$CaCl_2$	1.45	10.9	1.491			
Vermiculite/$MgSO_4$	0.41	3.6	2.054			
Vermiculite/$Ca(NO_3)_2$	1.52	2.4	1.274			
Vermiculite/$Li(NO_3)_2$	1.73	2.4	1.109			
Vermiculite/LiBr	1.94	1.9	1.172			
Vermiculite/63wt.% $LiNO_3$	0.4–0.5			< 0.5	33	[111]
Vermiculite	0.04	9	1.8		25	[112]
Vermiculite/57.3wt.% $CaCl_2$	1.13		1.55			
MCM-41	0.04	1137	1.3	0.3	20	[93]
MCM-41/3wt.% $Al2(SO_4)_3$	0.1	1021	1.12			
MCM-41/5wt.% $Al2(SO_4)_3$	0.15	993	1.12			
MCM-41/7wt.% $Al2(SO_4)_3$	0.17	941	1.01			
MCM-41		1050	1.1			[113]
MCM-41/37.7wt.% $CaCl_2$	0.7–0.75	325		0.7	20	
WSS	0.15	111.7	0.309	0.95	25	[114]
WSS/9.6wt.% LiCl	1.1	64.5	262			
WSS	0.15	111.7	0.309	0.95	25	[115]

Table 5 (continued)

Composite	Uptake (g g^{-1})	BET surface area (m^2 g^{-1})	V_{por} (cm^3 g^{-1})	P/P_s (–)	T_{ads} (°C)	Refs.
WSS/2.2wt.% $CaCl_2$	0.26	100.9	0.29			
WSS/13wt.% $CaCl_2$	0.66	49.9	0.209			
WSS/22.4wt.% $CaCl_2$	1.12	38.4	0.152			
WSS	0.26	149	0.37	0.95	25	[116]
WSS/5wt.% $CaCl_2$	0.31	119	0.33	0.95		
WSS/10wt.% $CaCl_2$	0.32	101	0.32	0.75		
WSS/5wt.% NaCl	0.35	129	0.33	0.95		
WSS/10wt.% NaCl	0.48	128	0.34	0.95		
WSS/5wt.% LiCl	0.38	124	0.33	0.95		
WSS/10wt.% LiCl	0.57	134	0.35	0.95		
SP	1.5	105.3	0.168	0.9	25	[117]
SP/$CaCl_2$	1.33	103.953	0.1657			

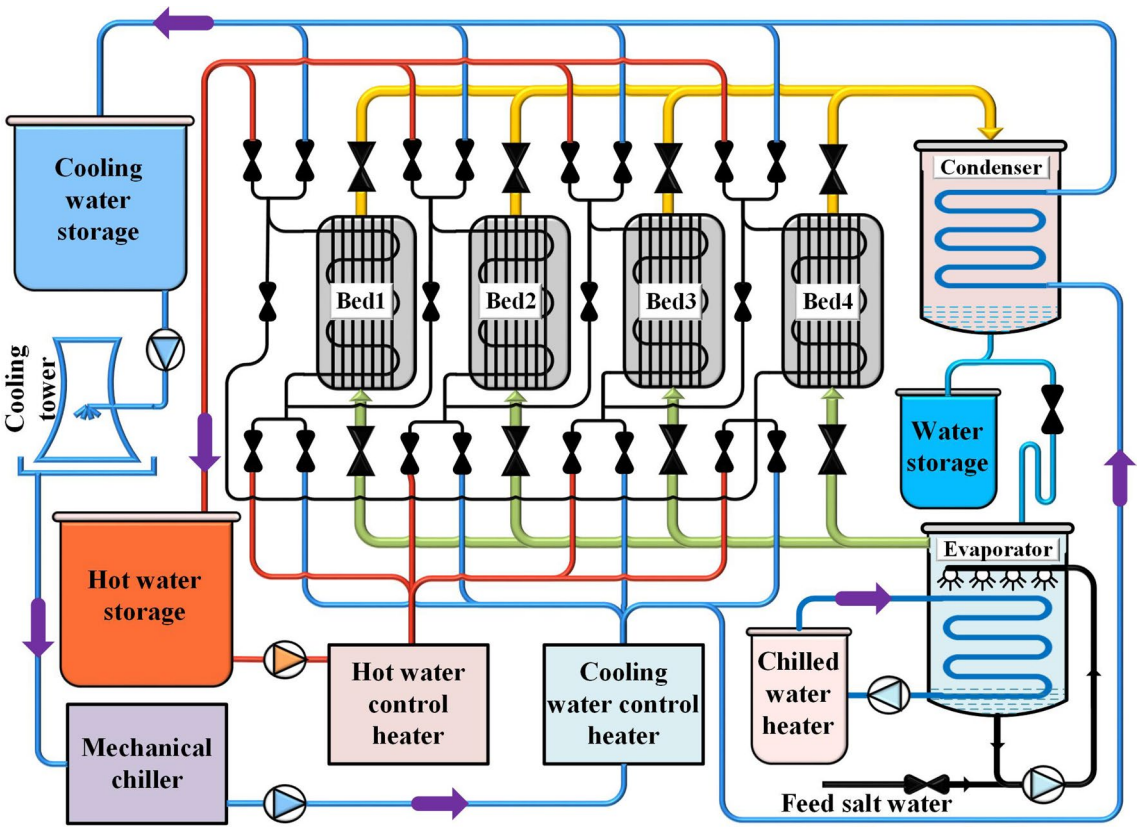

Fig. 4 Schematic diagram of the ADS used test facility [8]

or solar energy to generate potable. The study investigated a practical implementation of theoretical ADS cycles and their validity experimentally. As shown in Fig. 6, the study employed one adsorption unit with 2.124 kg of silica gel.

Ng et al. [120] analyzed the performance of ADS utilized by waste heat for producing desalinated water and cooling effect. A theoretical simulation for ADS was preceded. The cycle was explored using key performance parameters like

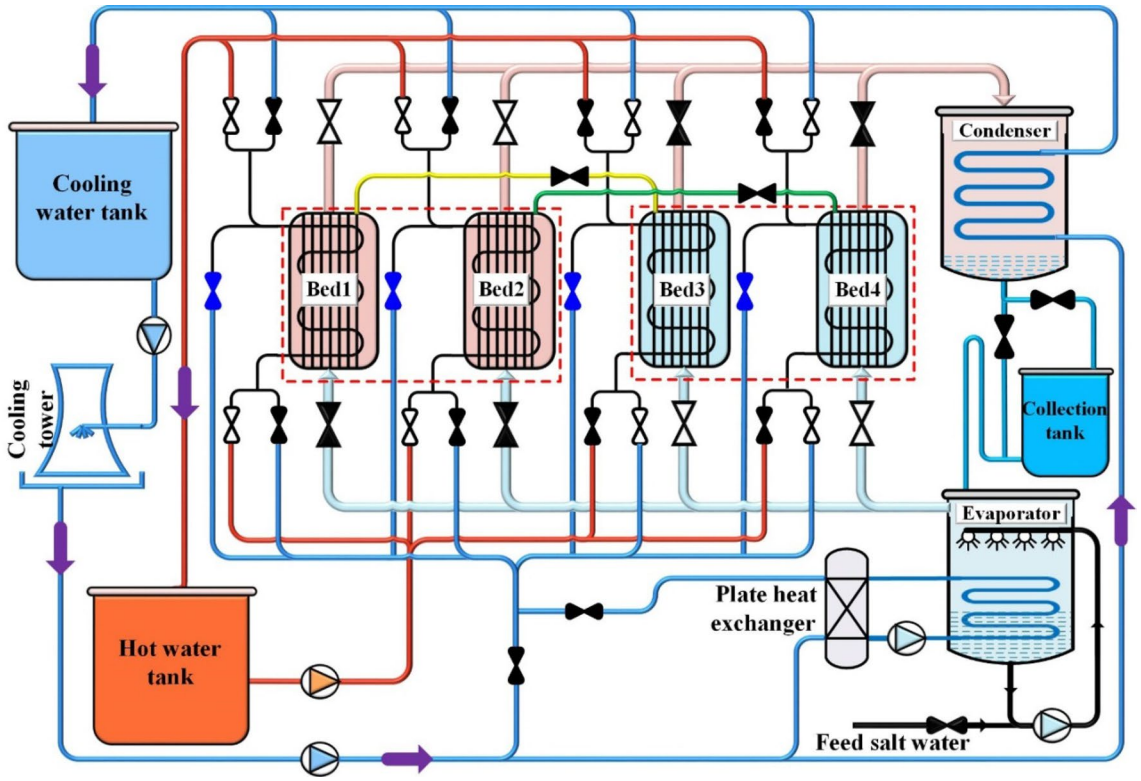

Fig. 5 Schematic diagram of used ADS experimental test rig stated in [118]

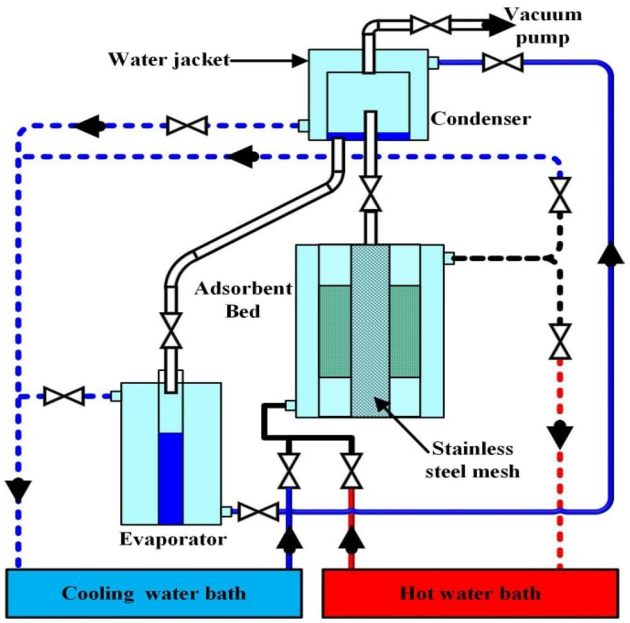

Fig. 6 One adsorption unit with 2.124 kg of silica gel [119]

(i) SCP, (ii) SDWP, (iii) COP, and (iv) overall conversion ratio (OCR). The mathematical results were certified by experimental data. Figure 7 expresses the advanced ADS cycle with 4 adsorption units with 36 kg silica gel per unit. At $T_{whi} = 85$ °C, the cycle produced 3.6 m^3 of desalinated water and 23 Raton at $T_{cho} = 10$ °C.

Mitra et al. [121] evaluated two-stage ADS for both cooling-cum-desalination. Figure 8 shows a schematic of the experimental facility. The study showed that a single-stage ADS system could not be used with an air-cooled condenser under tropical conditions, and this was realized by operating the system in a 2-stage model. Also, the study expressed a developed simulation model that was closer to experimental results than the previous one.

Gao et al. [122] investigated an innovative single-stage vacuum evaporator to extract saltwater. The system was settled to utilize an ultra-low-grade heat source of 50 °C. Figure 9 illustrates the investigated system. The adsorbent bed comprised 5 arrays of U-shaped aluminum finned tube heat-exchanger with 0.8 kg of silica gel (Type A). It was conducted that utilizing lower T_{cwi} enhanced the desorption process, which boosted the performance of the developed system.

Alsaman et al. [15] proposed and designed a new solar ADS for cooling and desalination. The proposed ADS was built and tested under Egypt's climate conditions. Figure 10

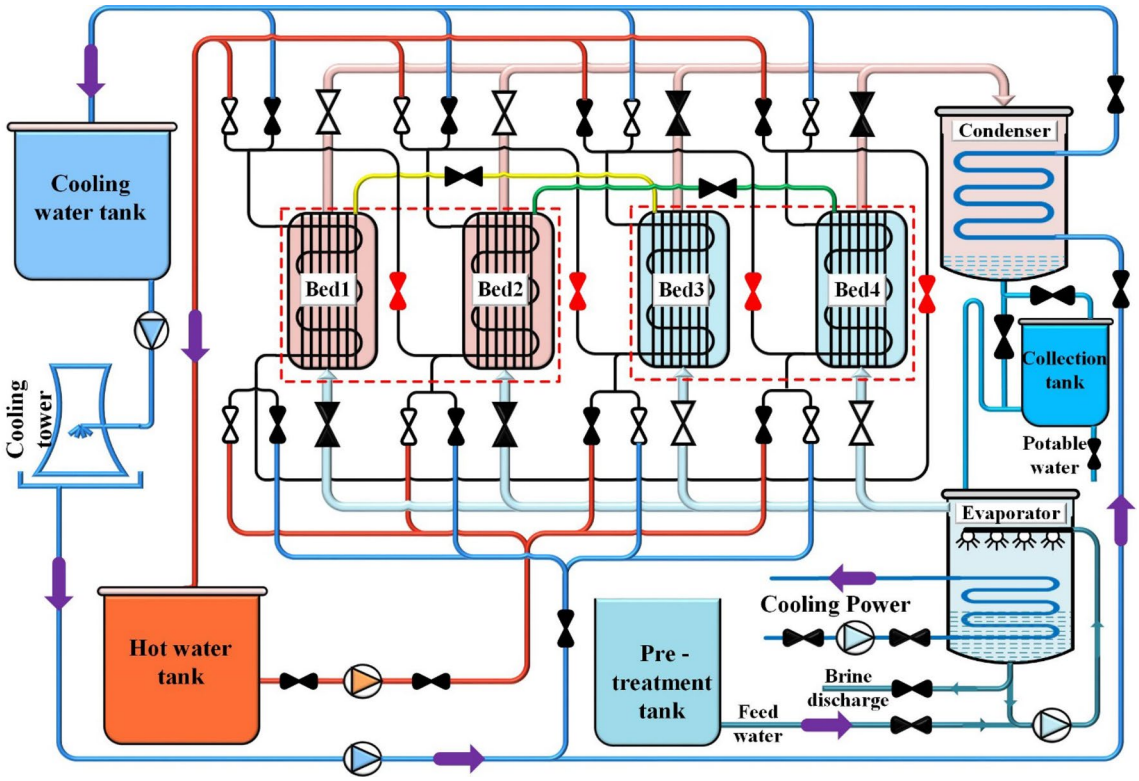

Fig. 7 Advanced ADS cycle with 4 adsorption units [120]

expresses the designed ADS 13.5 kg with silica gel. The Adsorption characteristics were also presented for the selected material. The theoretical model was close to experimental results. The results showed that SCP was 112 W/kg and SDWP was 4 m^3/day.ton with COP of 0.45. Dakkama et al. [74] investigated MOF development for producing ice and freshwater. Figure 11 expresses a schematic diagram of the investigated system. The adsorber bed contained 670 g of CPO-27 (Ni). Results indicated that the optimal operating salinity concentration was 35,000 ppm to produce ice (8.3 m^3/day/ton) with COP 0.9. The SDWP was 1.8 m^3/day/ton.

Youssef et al. [73] explored experimentally using CPO-27 (Ni) as adsorbent material for ADS applications. Experimental and numerical investigation for utilizing 0.67 kg of CPO-27(Ni) with a one-bed ADS system was obtained, as expressed in Fig. 12. Results demonstrated that by increasing T_{eva} and reducing T_{cond}, SCP was improved. The ADS created 65 Rton/ton at (T_{evap} = 20 °C). SDWP was improved to 22.8 m^3/ton.day at (T_{evap} = 40 °C, T_{con} = 5 °C and T_{des} = 95 °C). Olkis et al. [123–126] presented three papers illustrating the design of an experimental small-scale ADS desalinator for producing freshwater. The study introduced the world's smallest ADS with 0.2 kg silica gel, as shown in Fig. 12. The system achieved an SDWP of 7.7 kg/kg_{sg}. day. The ADS demonstrated the profits of heat combination between the adsorbent beds to reduce the consumed energy by 25% and raise the PR to 0.6.

Elsayed et al. [127] reported that MOF materials were recommended to substitute the traditional adsorbents. The study presented an experimental test of 0.375 kg aluminum fumarate in ADS. The performance of aluminum fumarate was higher than that of ADS utilizing silica gel and CPO-27(Ni) for desalination effect only at high P/P_s. Zhang et al. [128] presented a pilot-scale ADS with freshwater production of 100 kg/h, as illustrated in Fig. 13. The system was constructed based on small-scale system optimization and enhancement. The results exhibited that the desalinated water was less than 100 kg/h at T_{hwi} = 55 °C. At higher T_{hwi}, the desalinated water rate was improved to 191.3 kg/h at T_{hwi} = 80 °C.

Advanced experimental desalination investigations

In this section, the advanced adsorption desalination experimental investigations will be expressed. These experimental investigations are for only the desalination effect. In these systems, a heat recovery between evaporator and condenser

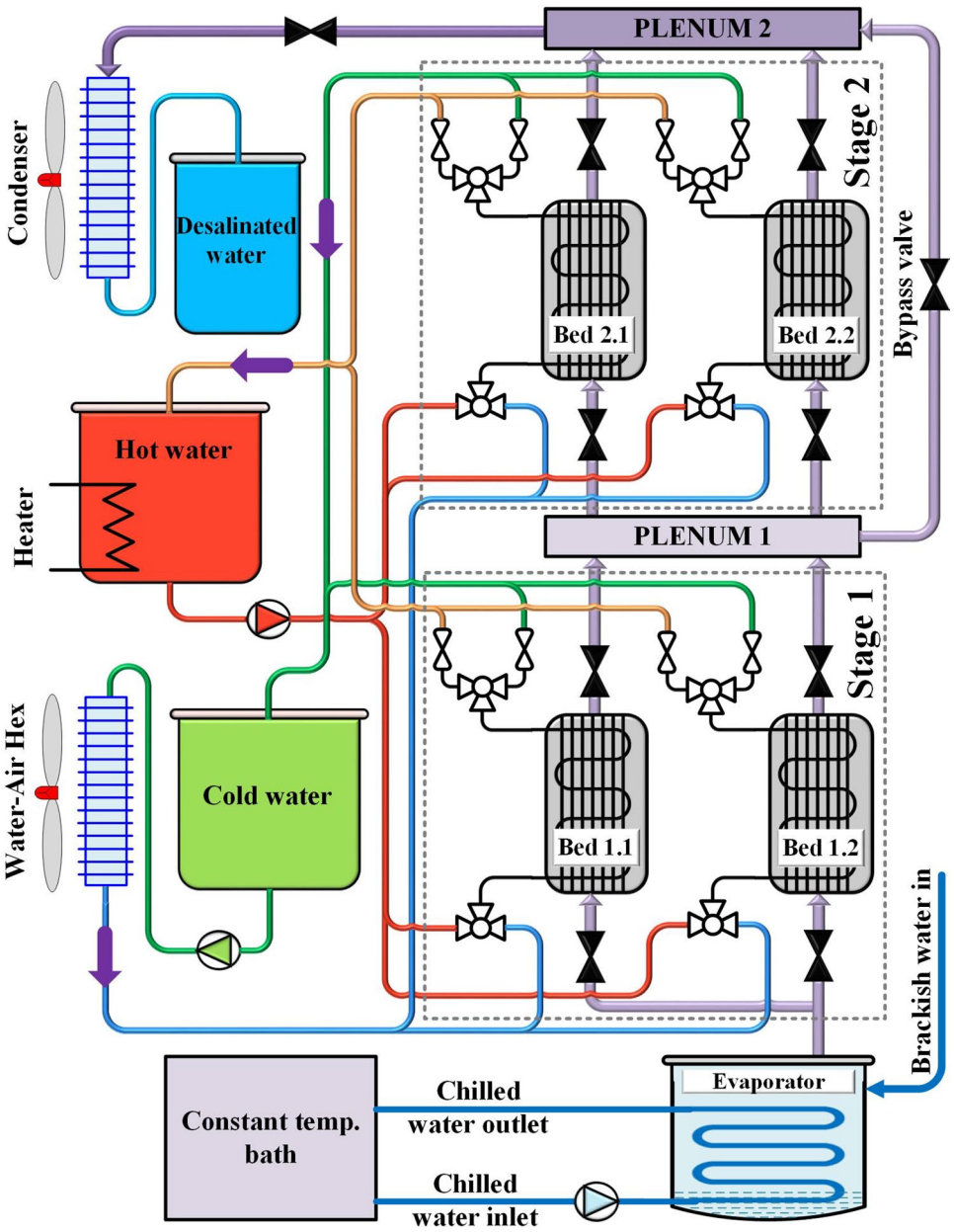

Fig. 8 Schematic of 2-bed two-stage ADS [121]

was utilized. Thu et al. [25]expressed the results of an investigation advanced AD cycle with internal heat recovery between condenser and evaporator. Figure 14 expresses the advanced AD cycle with 4 adsorption units with 36 kg silica gel per unit. A mathematically advanced AD cycle was developed and validated with experimental results. The advanced ADS could yield an SDWP of 9.24 m^3/ton daily at 70 °C with PR = 0.77. The proposed system could be operated at 50 °C T_{hwi} with SDWP 4.3. The advanced cycle SDWP was two times that of the traditional AD cycle.

Ma et al. [30] investigated an experimental heat recovery between adsorber and desorber beds for ADS with 29.17 kg silica gel per adsorption bed, as illustrated in Fig. 15. The results showed that the SDWP and PR were 4.69 and 0.766, respectively.

This heat recovery employment could not rise SDWP, but it could save consuming energy. Kim et al. [129] investigated the water quality measurements of AD plants. Feedwater was taken from the Red Sea. Figure 16 expresses the schematic AD cycle with 4 adsorption units. Water quality was assessed by complying with the Environmental Protection Agency (EPA) principles with major primary and minor inorganic drinking water contaminants and other usually tested water quality considerations. Desalinated water

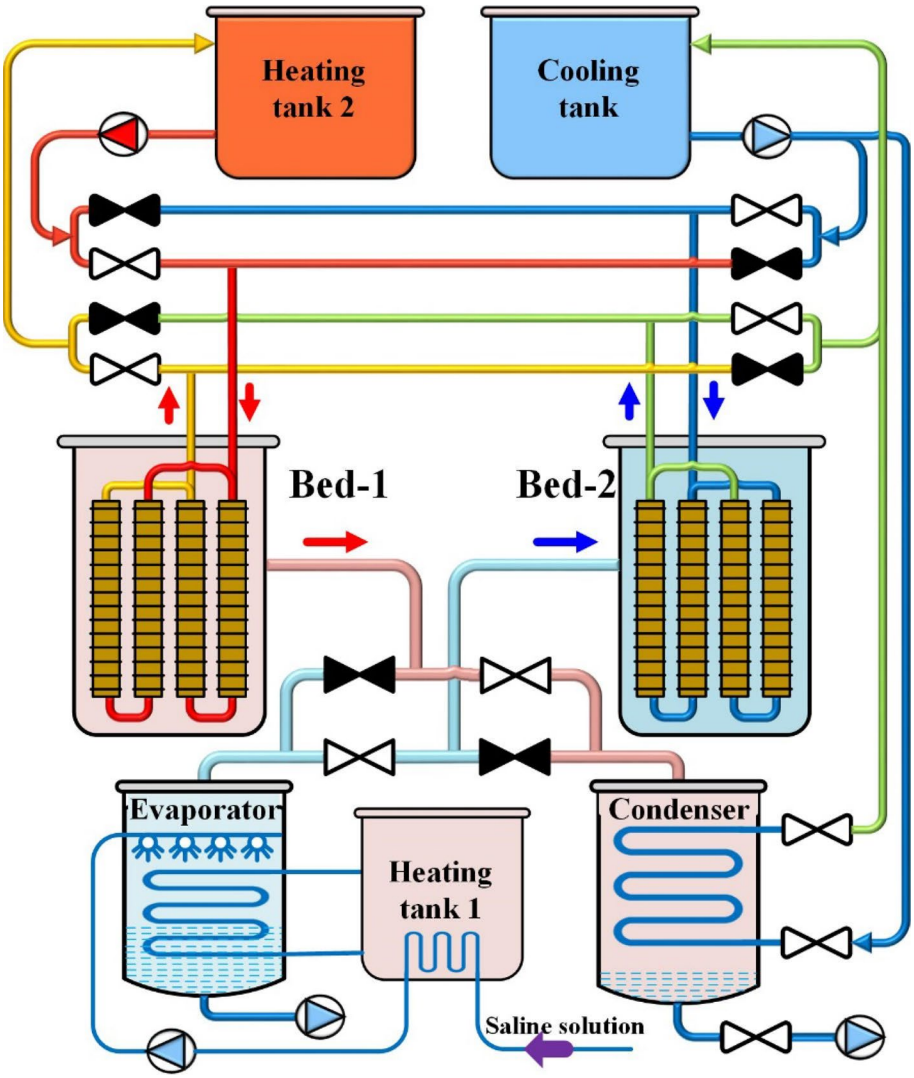

Fig. 9 Schematic of the used experimental facility [122]

testing ensured the good quality of generated freshwater. Test results showed that ADS effectively removes all forms of salts to less than 10 ppm. Bai et al. [29] investigated the mass recovery between adsorber and desorber beds for ADS and the feedwater quality effect on ADS performance. The results showed that the SDWP and SCP were 18.08 and 490, respectively.

Hybrid adsorption desalination with MED system

There are many studies on hybrid ADS with other systems such as RO-AD, AD-MVC, and AD-HDH. Still, many of these studies are theoretically investigated. The only experimental hybrid investigation systems were expressed between AD and MED. Shahzad et al. [130] presented an experimentally new hybrid "MEDAD" system, a coupling of the conventional MED and ADS, as expressed in Fig. 17. The main advantage of the MEDAD cycle is that it allowed some MED stages to work below ambient temperature, indifferent to the conventional MED. The hybrid system significantly increases desalinated water to 2.5–3 folds of conventional MED.

Son et al. [131] explored experimentally hybrid "MEDAD" desalination, applying synergetic impact for utilizing energy to improve the MEDAD performance, as expressed in Fig. 18. The MEDAD system significantly increased desalinated water up to 2–5 folds of conventional MED of the same rating.

Table 6 summarizes the results of previous experimental ADS studies. The SDWP for ADS that utilized silica gel varied from 3.6 to 14.2 m^3/day.ton. This wide range illustrates the significant effect of ADS system design and operating conditions. Therefore, the next section summarizes

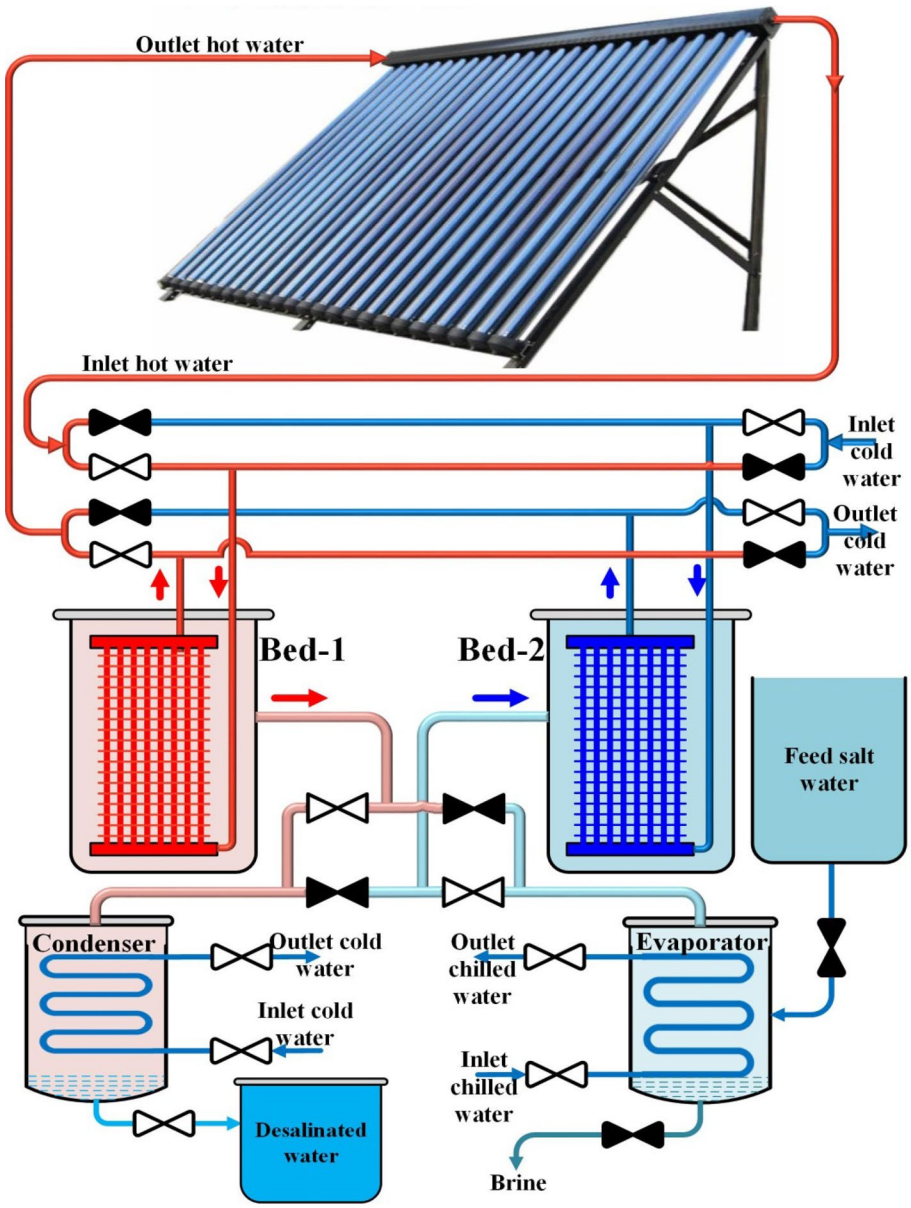

Fig. 10 Schematic diagram of the solar ADC test rig [15]

the heat exchanger configurations and their effect on ADS performance.

Effect of heat transfer of adsorption bed on ADS performance

In this section, the effect of heat transfers of adsorption bed on ADS performance. The current study expresses all adsorption desalination experimental investigations. The heat transfer parameters of adsorption beds are expressed in Table 7. The following equation illustrates heat transfer parameters.

To simplify the computation, the $TM_{inherent}$ of sorbed refrigerant was ignored. It is simplified in two ways: (1) the computed thermal mass no longer includes the sorbent's equilibrium composition, and (2) the thermal mass may be viewed as constant in sorption and desorption operations. Neglecting the TM of sorbed refrigerant will have a minor influence on TM_{total} for many adsorption heat exchangers (HXs).

The thermal mass of the adsorption bed is given by

$$TM_{total} = TM_{inherent} + TM_{design} \quad (1)$$

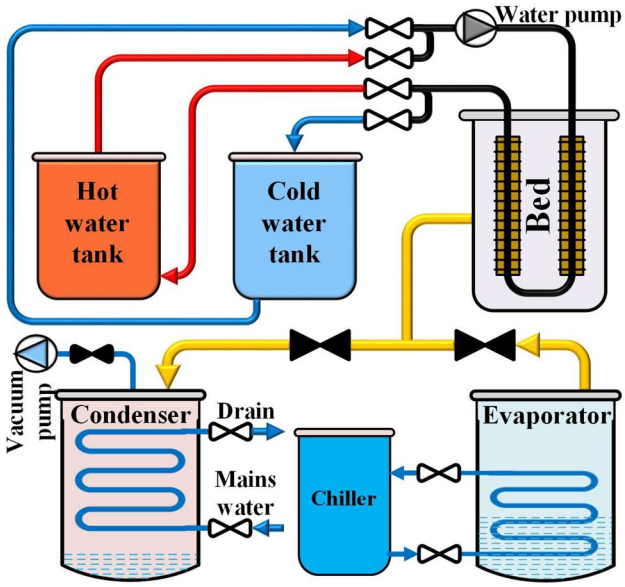

Fig. 11 Schematic diagram of ADS for ice making and freshwater [74]

$$TM_{inherent} = M_{adsorbent} Cp_{adsorbent} \quad (2)$$

$$TM_{design} = \rho_{HTF} V_{HTF} CP_{HTF} + \sum M_{metal} Cp_{metal} \quad (3)$$

where HTF represents heating thermal fluid.

The specific thermal mass is given by.

$$STM = \frac{TM_{design}}{M_{adsorbent}} \quad (4)$$

Figures 19 and 20 express the effect of bed design representing thermal masses of heat exchangers on ADS performance through the previous experimental studies. In the previous experimental studies, the STM varied from 1.74 to 6.58 kJ/kg. Figure 19 illustrates the COP variation by changing the adsorption bed's specific thermal mass (STM). The COP decreases from 0.766 to 0.36 with STM increasing 1.74–6.05 kJ/kg for silica gel adsorbent duo to increase the adsorption bed's thermal mass, which means more heat losses in the heating adsorption bed. This heat loss is represented in the heating of the heat exchanger. Figure 20 expresses the SDWP variation by changing the adsorption bed's specific thermal mass (STM). STM has a significant effect on SDWP. The SDWP increases from 3.6 to 18 m^3/day.ton (about 500% increasing) with STM increasing from 1.74 to 6.58 kJ/kg as a result of increasing the overall heat transfer coefficient due to increasing the thermal mass of the adsorption bed. This means more adsorbent vapor is released

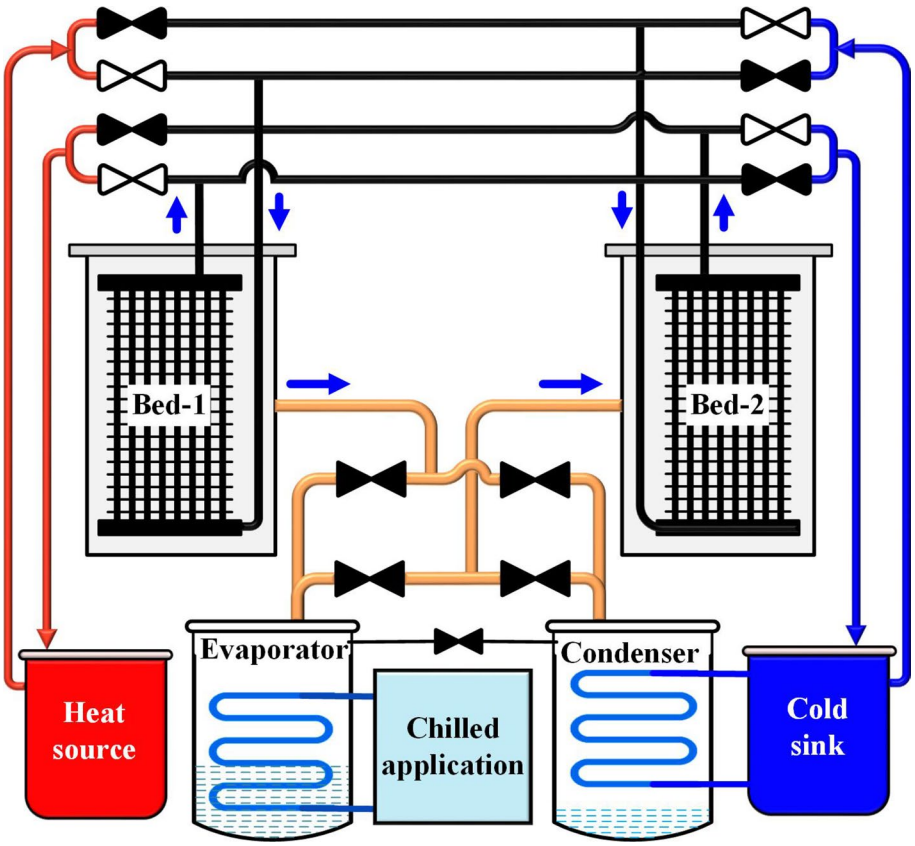

Fig. 12 Schematic diagram of small-scale ADS desalinator [123–125]

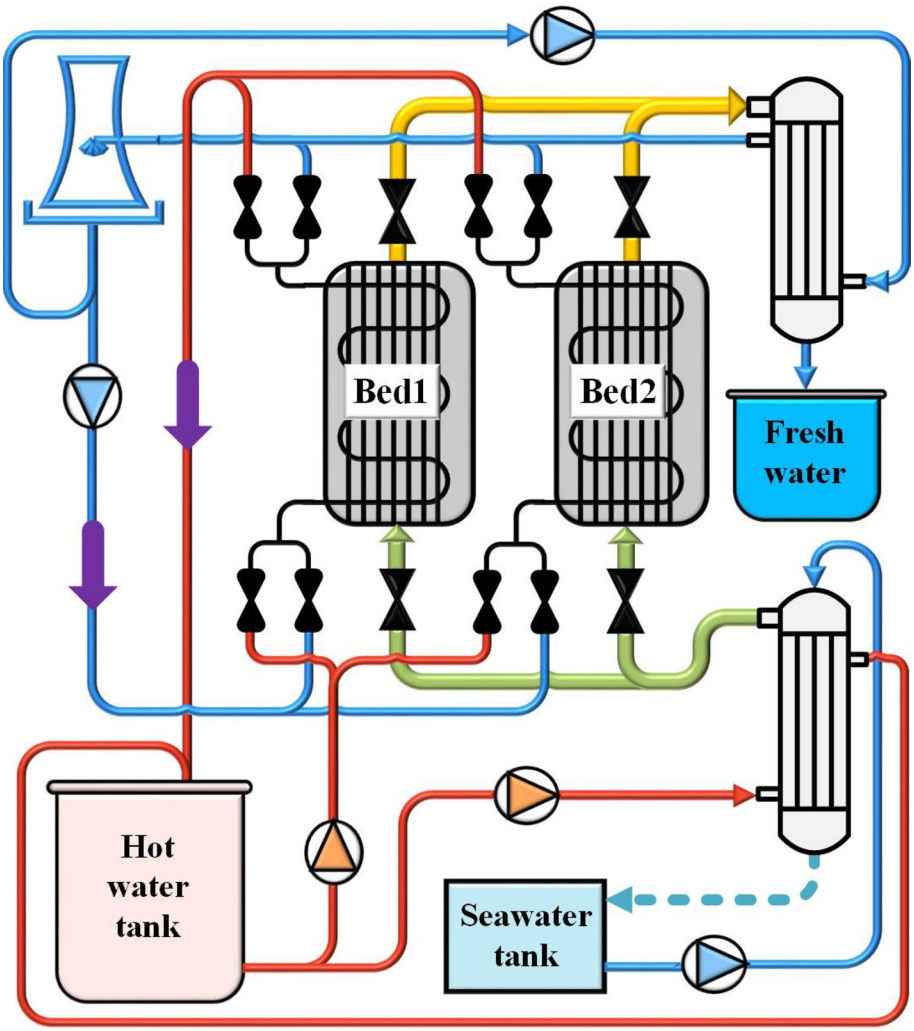

Fig. 13 Schematic diagram of pilot-scale ADS [76]

in desorption mode, leading to more desalinated water production in the condenser.

Challenges and perspectives

This section expresses the research gap, the required research topics in ADS, and future marketing challenges of marketing these ADS. Despite the many advantages of ADS, as they can be driven by renewable and/or waste energy, they still face difficulties in marketing and dissemination. This is because it suffers from high volume and relatively low efficiency compared to traditional devices, which decreases the productivity of these systems and makes them unattractive. Moreover, the number of experimental researches in this field is still limited compared to its importance. From this standpoint, it was necessary to show the gap and clarify the deficiency in this area. This is what this work is trying to show, as after reviewing the published research, it was found that the number of devices built to study desalination systems does not exceed a dozen. This clearly shows that the field still needs more effort, research, and the development of new methods and materials to raise the efficiency of this system. Therefore, it is recommended to do more experimental research to encourage the industrial sector and investors to build AD plants. The authors recommend these future researches focus on the following:-

1 Finding new adsorbent materials with a high adsorption capacity to reduce AD plant volume and increase performance in terms of SDWP and COP.
2 Finding new composite adsorbent materials for higher adsorption capacity

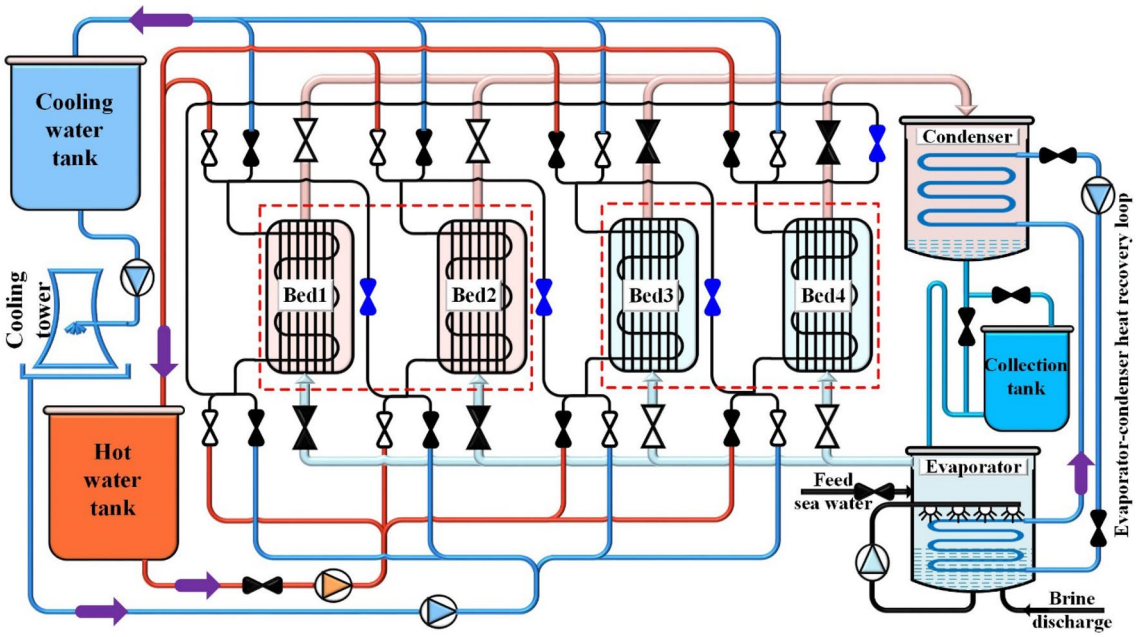

Fig. 14 Advanced ADS cycle with 4 adsorption units [25]

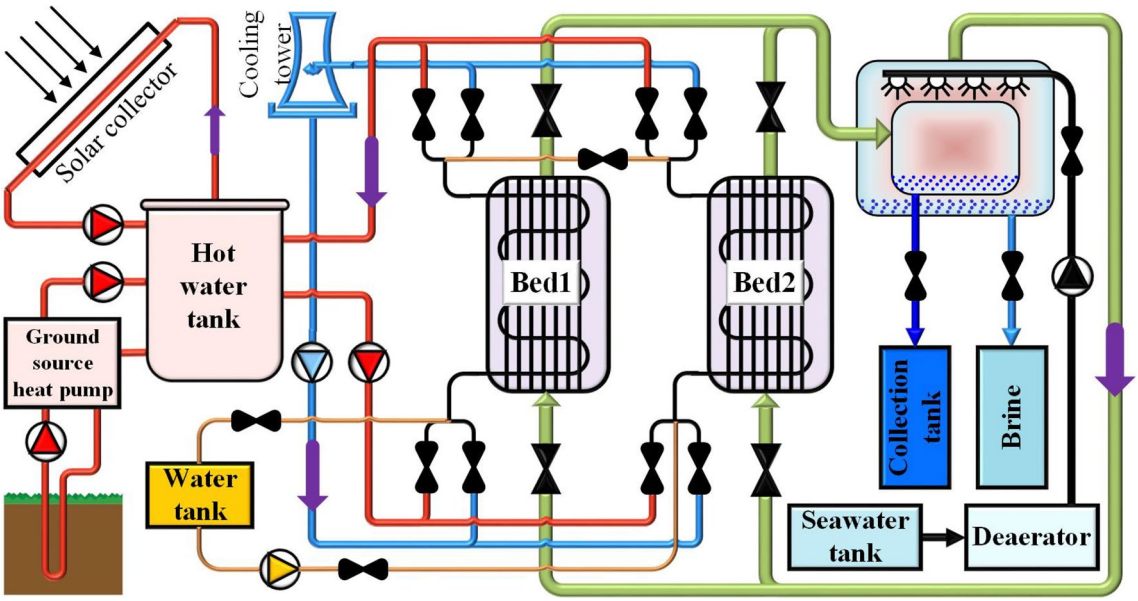

Fig. 15 Schematic diagram for heat recovery between adsorber and desorber beds [30]

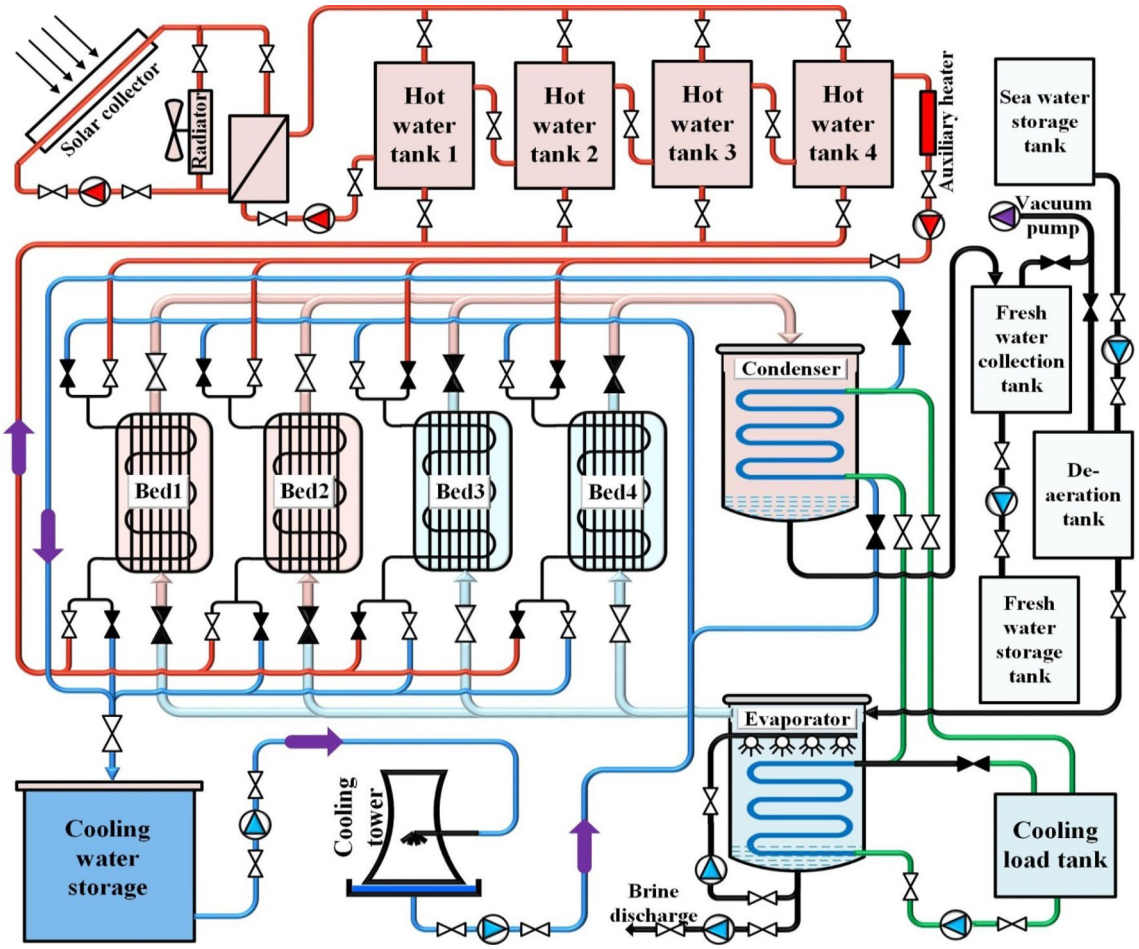

Fig. 16 schematic ADS cycle with 4 adsorption units [129]

3 How to increase the COP of the AD cycle by increasing the overall heat transfer coefficient of adsorption beds and evaporator and condenser.
4 Applying the recent theoretical research of ADS experimentally to close the gap between theoretical and experimental studies. Mathematical results [4–6, 24–28] achieved high values of SDWP and COP of 98 m^3/ton.day and 2.1, respectively [4]. However, this performance was not proven experimentally on either lab-scale, prototype, or pilot scale. Experimental measurements are still low as SDWP did not increase more than 18 m^3/ton.day, and COP did not increase than 0.78.
5 Applying the theoretical hybridization between ADS and RO, HDH, salt hydrate, and absorption system experimentally to realize the benefits of these combinations. Also, study new combinations of ADS and other desalination systems.
6 Establish more pilot plants and scale up adsorption desalination plants to encourage the industrial sector to invest in these ADS. Finding new adsorbent materials with a high adsorption capacity to reduce AD plant volume and increase performance in terms of SDWP and COP.

Conclusions

This review presents a survey about the constructed and tested experimental water distillation systems that consider adsorption technology. Not so many systems have been found, as less than ten systems were built worldwide to take off freshwater from the salty water by adsorption evaporation technology. One of these few systems had been built in Egypt. The majority of these systems

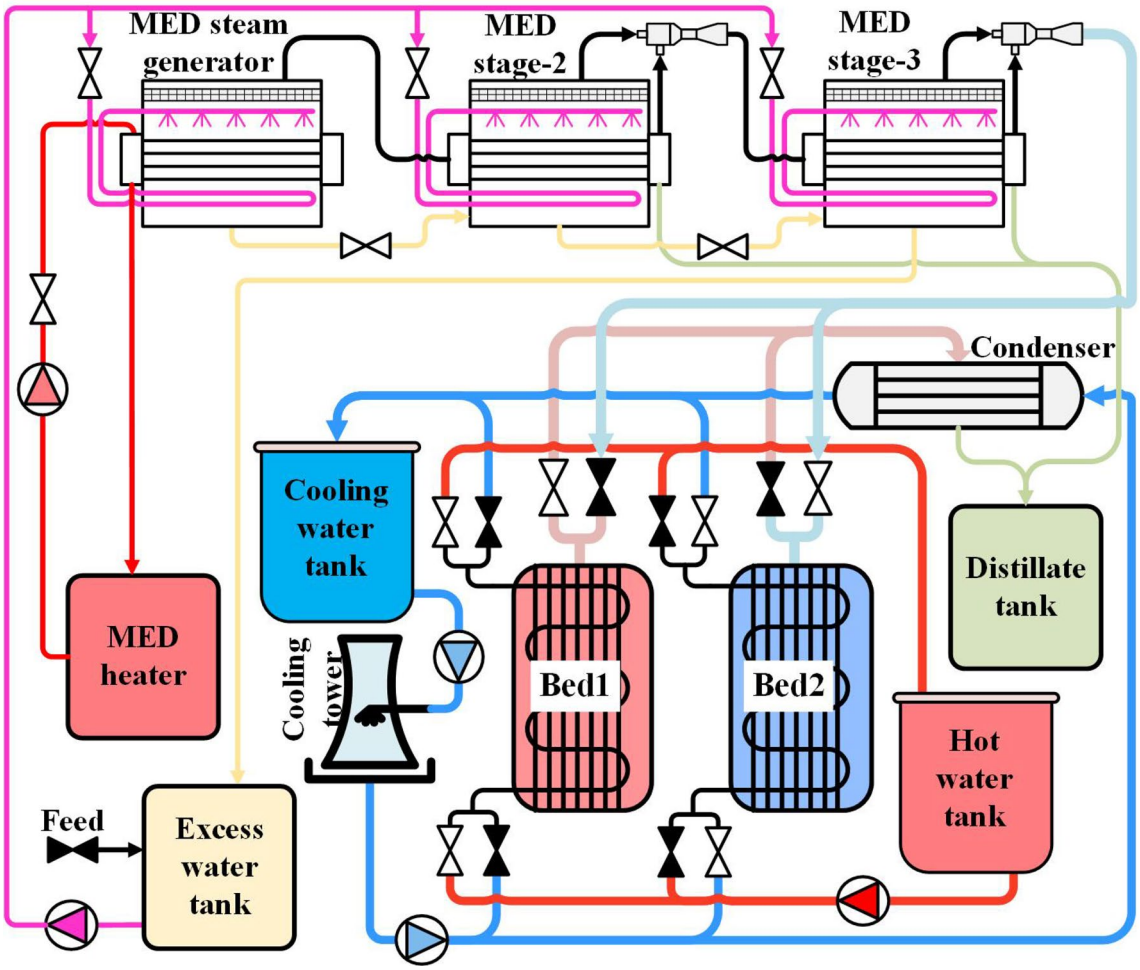

Fig. 17 MEDAD schematic diagram for experimental rig installed in NUS [130]

employed silica gel as an adsorbent material; its composites and metal–organic framework were also used. The amounts of the used adsorbents varied from less than 1 kg, reaching 1440 kg. Produced amount of pure water per day per ton of adsorbent has been varied as well, from 1.8 m^3/ton/day up to 25 m^3/ton/day. The whole presented system used a fin tube-type heat exchanger. It is clear that the technology is still in the cradle, and more experimental test rigs are required to be built and tested at different operating conditions. Also, more adsorbent materials are needed to be employed in such systems.

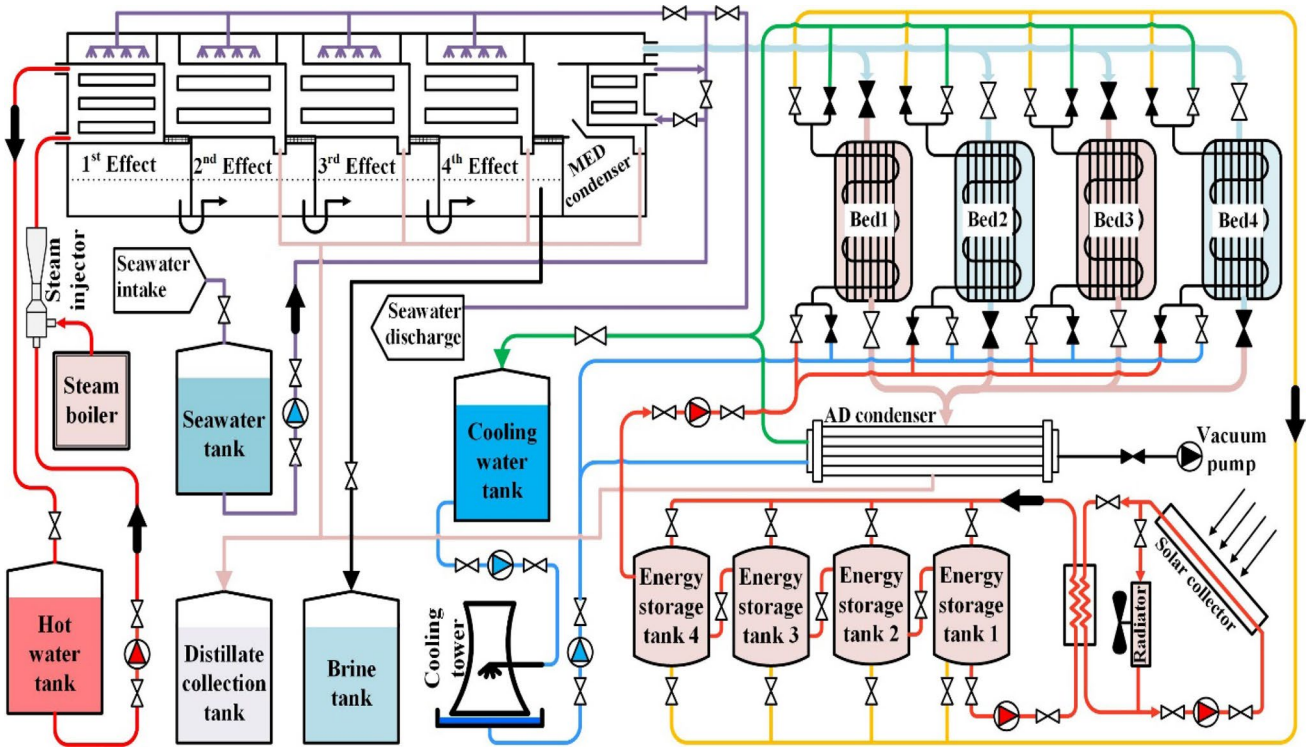

Fig. 18 Pictorial view of MED-AD system [131]

Table 6 Comparison between previous experimental ADS studies

Adsorbent material	Half cycle time (s)	No. of bed	Adsorbent weight (kg)	T_{cw} (°C)	T_{hw} (°C)	SDWP (m^3/ton)	SCP (W/kg)	COP (–)	Refs.
Silica gel	180	4	36	30	85	4.7	–	0.28	[8]
Silica gel	650	2	6.75	30	85	4	112	0.45	[15]
Silica gel	600	4	36	30	85	14.2	–	0.74	[25]
Silica gel	900	2	29.17	27	83	4.69	–	0.766	[30]
Silica gel	600	4/2	36	30	85	10	–	0.61	[118]
Silica gel	480	4	36	29.5	85	8	181	–	[120]
Silica gel	1200	2	0.2	25	80	7.7	80	0.6	[123–126]
Silica gel	900	2	1440	27	80	3.6	–	0.72	[128]
CPO-27Ni MOF	720	1	0.670	20	110	6.9	200	–	[73, 132, 133]
CPO-27Ni MOF	900	1	0.670	24	95	1.8	–	0.48	[74]
Aluminum fumarate	900	2	0.375	30	90	8.5	250	0.13	[127]
Aluminum fumarate	250	2	23.2	25	85	8.66	226	0.5	[134]
Aluminum fumarate	500	1	0.3	30	90	14.4	549.7	0.26	[135]
Montmorillonite/HCl	450	2	2.65	25	85	4.4	110	0.41	[12]
MWCNT embedded zeolite13X/$CaCl_2$	542	2	1.1	24	85	18.08	490	0.3	[29]

Table 7 The heat transfer parameters of adsorption beds for different excremental test rigs

Component (section) shape of HX	Working pair	Heat transfer fluid	Sorbent mass (kg)	HX Mass (kg)	TM_{total} (kJ/K)	$m_{sorb}/m_{H.X}$	STM (TM/$m_{sorb.}$)	Refs.
Tube fin HX packed	Silica gel/water	Water	6.75	25.44	16.2	0.26533	2.4	[15]
Tube fin HX packed	Silica gel/water	Water	0.21	0.81	0.737	0.259259	3.5	[123–126]
Tube fin HX packed	Silica gel/water	Water	29.17	60.34	50.83	0.483427	1.74	[30]
Tube fin HX packed	Silica gel/water	Water	36	–	184.1	–	5.11	[120]
Tube fin HX packed	Silica gel/water	Water	1440	1293.6	2458.8	1.082251	1.756	[128]
Shell and tube HX stage 1	Silica gel/water	Water	5.6	25	17.152	0.224	3.06	[121]
Shell and tube HX stage 2	Silica gel/water	Water	3.2	22	13.5	0.145455	4.22	[121]
Tube fin HX packed	Silica gel/water	Water	36	–	217.22	–	6.03	[25]
Tube fin HX packed	CPO-27Ni MOF/water	Water	0.67	29.97	–	0.022356	–	[73, 132, 133]
Tube fin HX packed	MWCNT embedded zeolite13X/$CaCl_2$	Water	1.1	8	7.24	0.137	6.58	[29]
Tube fin HX packed	Montmorillonite/HCl	Water	2.65	12.97	8.19	0.204	3.09	[12]

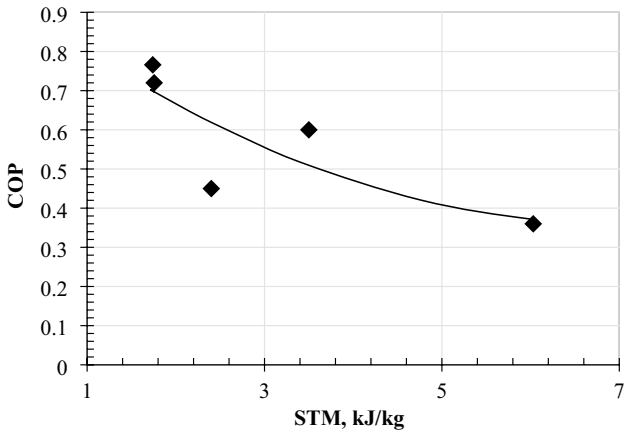

Fig. 19 Effect of STM on COP of ADS

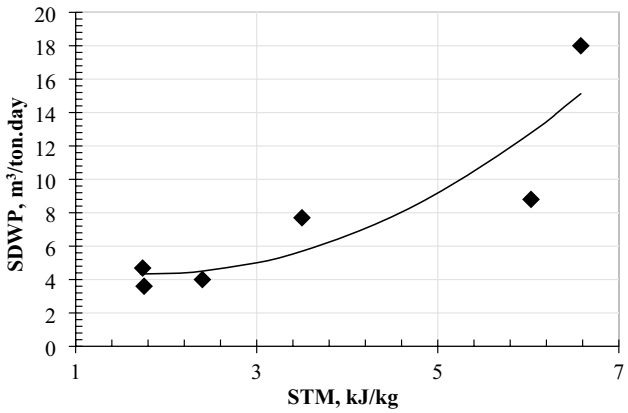

Fig. 20 Effect of STM on SDWP of ADS

Acknowledgements This research is a part of a research project supported by the Academy of Scientific Research and Technology (ASRT) through call Egypt scientists -2. Call no. 2/2019/ASRT-Nexus.

Declarations

Conflict of interest The authors declare that they have no conflict of interest.

References

1. Harby, K., Ali, E.S., Almohammadi, K.M.: A novel combined reverse osmosis and hybrid absorption desalination-cooling system to increase overall water recovery and energy efficiency. J. Clean. Prod. **287**, 125014 (2021). https://doi.org/10.1016/j.jclepro.2020.125014
2. Thu, K., Chakraborty, A., Kim, Y.D., Myat, A., Saha, B.B., Ng, K.C.: Numerical simulation and performance investigation of an advanced adsorption desalination cycle. Desalination **308**, 209–218 (2013). https://doi.org/10.1016/j.desal.2012.04.021
3. Sadri, S., Khoshkhoo, R.H., Ameri, M.: Optimum exergo-economic modeling of novel hybrid desalination system (MEDAD+RO). Energy **149**, 74–83 (2018). https://doi.org/10.1016/j.energy.2018.02.006
4. Ali, E.S., Mohammed, R.H., Qasem, N.A.A., Zubair, S.M., Askalany, A.: Solar-powered ejector-based adsorption desalination system integrated with a humidification-dehumidification system. Energy Convers. Manag. **238**, 114113 (2021). https://doi.org/10.1016/j.enconman.2021.114113
5. Ali, E.S., Mohammed, R.H., Askalany, A.: A daily freshwater production of 50 m3/ton of silica gel using an adsorption-ejector combination powered by low-grade heat. J. Clean. Prod. **282**, 124494 (2021). https://doi.org/10.1016/j.jclepro.2020.124494
6. Askalany, A.A., Ali, E.S.: A new approach integration of ejector within adsorption desalination cycle reaching COP higher than one. Sustain. Energy Technol. Assess. **41**, 100766 (2020). https://doi.org/10.1016/j.seta.2020.100766
7. Ng, K.C., Shahzad, M.W., Son, H.S., Hamed, O.A.: An exergy approach to efficiency evaluation of desalination. Appl. Phys. Lett. **110**, 184101 (2017). https://doi.org/10.1063/1.4982628
8. Wang, X., Ng, K.C.: Experimental investigation of an adsorption desalination plant using low-temperature waste heat. Appl. Therm. Eng. **25**, 2780–2789 (2005). https://doi.org/10.1016/j.applthermaleng.2005.02.011
9. Shemer, H., Semiat, R.: Sustainable RO desalination – Energy demand and environmental impact. Desalination **424**, 10–16 (2017). https://doi.org/10.1016/j.desal.2017.09.021
10. Ding, D., Huang, J., Deng, X., Fu, K.: Recent advances and perspectives of nanostructured amorphous alloys in electrochemical water electrolysis. Energy Fuels **35**, 15472–15488 (2021). https://doi.org/10.1021/acs.energyfuels.1c02706
11. Kim, Y.D., Woo, S.Y., Lee, H.S., Ji, H.: Adsorption isotherm model for analyzing the adsorption characteristics of water vapor to commercially available silica gel adsorbents for adsorption desalination applications. J. Chem. Eng. Data. **66**, 1144–1156 (2021). https://doi.org/10.1021/acs.jced.0c00927
12. Ali, E.S., Askalany, A.A., Harby, K., Diab, M.R., Hussein, B.R.M., Alsaman, A.S.: Experimental adsorption water desalination system utilizing activated clay for low grade heat source applications. J. Energy Storage **43**, 103219 (2021). https://doi.org/10.1016/j.est.2021.103219
13. Yang, M., Wang, X., Li, J., Zheng, J.N., Jiang, L.: Effects of particle sizes on growth characteristics of propane hydrate in uniform/nonuniform sands for desalination application. Energy Fuels **36**, 1003–1014 (2022). https://doi.org/10.1021/acs.energyfuels.1c03709
14. Ali, E.S., Askalany, A.A., Harby, K., Diab, M.R., Alsaman, A.S.: Adsorption desalination-cooling system employing copper sulfate driven by low grade heat sources. Appl. Therm. Eng. **136**, 169–176 (2018). https://doi.org/10.1016/j.applthermaleng.2018.03.014
15. Alsaman, A.S., Askalany, A.A., Harby, K., Ahmed, M.S.: Performance evaluation of a solar-driven adsorption desalination-cooling system. Energy **128**, 196–207 (2017). https://doi.org/10.1016/j.energy.2017.04.010
16. Amin, Z.M., Hawlader, M.N.A.: Analysis of solar desalination system using heat pump. Renew. Energy **74**, 116–123 (2015). https://doi.org/10.1016/j.renene.2014.07.028
17. Ali, E.S., Mohammed, R.H., Zohir, A.E., Farid, A.M., Elshaer, R.N., El-Ghetany, H.H., Askalany, A.A.: Novel ultrasonic dynamic vapor sorption apparatus for adsorption drying, cooling and desalination applications. Energy Rep. **8**, 8798–8804 (2022). https://doi.org/10.1016/j.egyr.2022.06.026
18. Askalany, A., Habib, K., Ghazy, M., Assadi, M.K.: Adsorption cooling system employing activated carbon/ hfc410a adsorption pair. ARPN J. Eng. Appl. Sci. **11**, 12253–12257 (2016)
19. Ghazy, M., Askalany, A.A., Ibrahim, E.M.M., Mohamed, A.S.A., Ali, E.S., AL-Dadah, R.: Solar powered adsorption desalination system employing CPO-27(Ni). J. Energy Storage **53**, 105174 (2022). https://doi.org/10.1016/j.est.2022.105174
20. Ghazy, M., Ibrahim, E.M.M., Mohamed, A.S.A., Askalany, A.A.: Cooling technologies for enhancing photovoltaic–thermal (PVT) performance: a state of the art. Int. J. Energy Environ. Eng. (2022). https://doi.org/10.1007/s40095-022-00491-8
21. Ghazy, M., Askalany, A., Kamel, A., Khalil, K.M.S., Mohammed, R.H., Saha, B.B.: Performance enhancement of adsorption cooling cycle by pyrolysis of Maxsorb III activated carbon with ammonium carbonate. Int. J. Refrig. **126**, 210–221 (2021). https://doi.org/10.1016/j.ijrefrig.2020.12.036
22. Askalany, A.A., Saha, B.B.: Towards an accurate estimation of the isosteric heat of adsorption—a correlation with the potential theory. J. Colloid Interface Sci. **490**, 59–63 (2017). https://doi.org/10.1016/j.jcis.2016.11.040
23. Zejli, D., Benchrifa, R., Bennouna, A., Bouhelal, O.K.: A solar adsorption desalination device: first simulation results. Desalination **168**, 127–135 (2004). https://doi.org/10.1016/j.desal.2004.06.178
24. Thu, K., Yanagi, H., Saha, B.B., Ng, K.C.: Performance investigation on a 4-bed adsorption desalination cycle with internal heat recovery scheme. Desalination **402**, 88–96 (2017). https://doi.org/10.1016/j.desal.2016.09.027
25. Thu, K., Saha, B.B., Chakraborty, A., Chun, W.G., Ng, K.C.: Study on an advanced adsorption desalination cycle with evaporator-condenser heat recovery circuit. Int. J. Heat Mass Transf. **54**, 43–51 (2011). https://doi.org/10.1016/j.ijheatmasstransfer.2010.09.065
26. Ali, E.S., Askalany, A.A., Zohir, A.E.: Innovative employing of salt hydration with adsorption to enhance performance of desalination and heat transformation systems. Appl. Therm. Eng. **179**, 115614 (2020). https://doi.org/10.1016/j.applthermaleng.2020.115614
27. Askalany, A., Ali, E.S., Mohammed, R.H.: A novel cycle for adsorption desalination system with two stages-ejector for higher water production and efficiency. Desalination **496**, 114753 (2020). https://doi.org/10.1016/j.desal.2020.114753
28. Ali, E.S., Muhammad Asfahan, H., Sultan, M., Askalany, A.A.: A novel ejectors integration with two-stages adsorption

desalination: away to scavenge the ambient energy. Sustain. Energy Technol. Assess. **48**, 101658 (2021). https://doi.org/10.1016/j.seta.2021.101658
29. Bai, S., Ho, T.C., Ha, J., An, A.K., Tso, C.Y.: Study of the salinity effects on the cooling and desalination performance of an adsorption cooling cum desalination system with a novel composite adsorbent. Appl. Therm. Eng. **181**, 115879 (2020). https://doi.org/10.1016/j.applthermaleng.2020.115879
30. Ma, H., Zhang, J., Liu, C., Lin, X., Sun, Y.: Experimental investigation on an adsorption desalination system with heat and mass recovery between adsorber and desorber beds. Desalination **446**, 42–50 (2018). https://doi.org/10.1016/j.desal.2018.08.022
31. Askalany, A.A., Ernst, S.J., Hügenell, P.P.C., Bart, H.J., Henninger, S.K., Alsaman, A.S.: High potential of employing bentonite in adsorption cooling systems driven by low grade heat source temperatures. Energy **141**, 782–791 (2017). https://doi.org/10.1016/j.energy.2017.07.171
32. White, J.: A CFD simulation on how the different sizes of silica gel will affect the adsorption performance of silica gel. Model. Simul. Eng. **2012**, 1–12 (2012). https://doi.org/10.1155/2012/651434
33. Thu, K., Chakraborty, A., Saha, B.B., Ng, K.C.: Thermo-physical properties of silica gel for adsorption desalination cycle. Appl. Therm. Eng. **50**, 1596–1602 (2013). https://doi.org/10.1016/j.applthermaleng.2011.09.038
34. Robens, E., Wang, X.: Investigation on the isotherm of silica gel+water systems. J. Therm. Anal. Calorim. **76**, 659–669 (2004). https://doi.org/10.1023/b:jtan.0000028045.96239.7e
35. Mohammed, R.H., Mesalhy, O., Elsayed, M.L., Su, M., Chow, C.L.: Revisiting the adsorption equilibrium equations of silica-gel/water for adsorption cooling applications. Int. J. Refrig. **86**, 40–47 (2018). https://doi.org/10.1016/j.ijrefrig.2017.10.038
36. Alsaman, A.S., Ibrahim, E.M.M., Ahmed, M.S., Askalany, A.A.: Composite adsorbent materials for desalination and cooling applications: a state of the art. Int. J. Energy Res. **46**, 10345–10371 (2022). https://doi.org/10.1002/er.7894
37. Bahgaat, A.K., Hassan, H.E., Melegy, A.A., Abd-El Kareem, A.M., Mohamed, M.H.: Synthesis and characterization of zeolite-Y from natural clay of Wadi Hagul Egypt. Egypt J Chem **63**, 3791–3800 (2020). https://doi.org/10.21608/EJCHEM.2020.23195.2378
38. Sayilgan, ŞÇ., Mobedi, M., Ülkü, S.: Effect of regeneration temperature on adsorption equilibria and mass diffusivity of zeolite 13x-water pair. Microporous Mesoporous Mater. **224**, 9–16 (2016). https://doi.org/10.1016/j.micromeso.2015.10.041
39. Kayal, S., Baichuan, S., Saha, B.B.: Adsorption characteristics of AQSOA zeolites and water for adsorption chillers. Int. J. Heat Mass Transf. **92**, 1120–1127 (2016). https://doi.org/10.1016/j.ijheatmasstransfer.2015.09.060
40. Teo, H.W.B., Chakraborty, A., Han, B.: Water adsorption on CHA and AFI types zeolites: modelling and investigation of adsorption chiller under static and dynamic conditions. Appl. Therm. Eng. **127**, 35–45 (2017). https://doi.org/10.1016/j.applthermaleng.2017.08.014
41. Henninger, S.K., Schmidt, F.P., Henning, H.M.: Water adsorption characteristics of novel materials for heat transformation applications. Appl. Therm. Eng. **30**, 1692–1702 (2010). https://doi.org/10.1016/j.applthermaleng.2010.03.028
42. Chaemchuen, S., Xiao, X., Klomkliang, N., Yusubov, M., Verpoort, F.: Tunable metal-organic frameworks for heat transformation applications. Nanomaterials **8**, 661 (2018). https://doi.org/10.3390/nano8090661
43. Tatlier, M., Munz, G., Henninger, S.K.: Relation of water adsorption capacities of zeolites with their structural properties. Microporous Mesoporous Mater. **264**, 70–75 (2018). https://doi.org/10.1016/j.micromeso.2017.12.031
44. Furukawa, H., Gándara, F., Zhang, Y.B., Jiang, J., Queen, W.L., Hudson, M.R., Yaghi, O.M.: Water adsorption in porous metal-organic frameworks and related materials. J. Am. Chem. Soc. **136**, 4369–4381 (2014). https://doi.org/10.1021/ja500330a
45. Canivet, J., Bonnefoy, J., Daniel, C., Legrand, A., Coasne, B., Farrusseng, D.: Structure-property relationships of water adsorption in metal-organic frameworks. New J. Chem. **38**, 3102–3111 (2014). https://doi.org/10.1039/c4nj00076e
46. Burtch, N.C., Jasuja, H., Walton, K.S.: Water stability and adsorption in metal-organic frameworks. Chem. Rev. **114**, 10575–10612 (2014). https://doi.org/10.1021/cr5002589
47. Administrator, O.J.S.T.: Metal-organic frameworks applied for water purification. Resour Technol (2018). https://doi.org/10.18799/24056537/2018/1/177
48. Taylor, J.M., Vaidhyanathan, R., Iremonger, S.S., Shimizu, G.K.H.: Enhancing water stability of metal-organic frameworks via phosphonate monoester linkers. J. Am. Chem. Soc. **134**, 14338–14340 (2012). https://doi.org/10.1021/ja306812r
49. Canivet, J., Fateeva, A., Guo, Y., Coasne, B., Farrusseng, D.: Water adsorption in MOFs: fundamentals and applications. Chem. Soc. Rev. **43**, 5594–5617 (2014). https://doi.org/10.1039/c4cs00078a
50. Jasuja, H., Burtch, N.C., Huang, Y.G., Cai, Y., Walton, K.S.: Kinetic water stability of an isostructural family of zinc-based pillared metal-organic frameworks. Langmuir **29**, 633–642 (2013). https://doi.org/10.1021/la304204k
51. Li, S., Chen, Y., Pei, X., Zhang, S., Feng, X., Zhou, J., Wang, B.: Water purification: adsorption over metal-organic frameworks. Chin J. Chem. **34**, 175–185 (2016). https://doi.org/10.1002/cjoc.201500761
52. Li, N., Xu, J., Feng, R., Hu, T.L., Bu, X.H.: Governing metal-organic frameworks towards high stability. Chem. Commun. **52**, 8501–8513 (2016). https://doi.org/10.1039/c6cc02931k
53. Towsif Abtab, S.M., Alezi, D., Bhatt, P.M., Shkurenko, A., Belmabkhout, Y., Aggarwal, H., Weseliński, ŁJ., Alsadun, N., Samin, U., Hedhili, M.N., Eddaoudi, M.: Reticular chemistry in action: a hydrolytically stable mof capturing twice its weight in adsorbed water. Chem. **4**, 94–105 (2018). https://doi.org/10.1016/j.chempr.2017.11.005
54. Reinsch, H., Marszalek, B., Wack, J., Senker, J., Gil, B., Stock, N.: A new Al-MOF based on a unique column-shaped inorganic building unit exhibiting strongly hydrophilic sorption behaviour. Chem. Commun. **48**, 9486–9488 (2012). https://doi.org/10.1039/c2cc34909d
55. Reinsch, H., van der Veen, M.A., Gil, B., Marszalek, B., Verbiest, T., de Vos, D., Stock, N.: Structures, sorption characteristics, and nonlinear optical properties of a new series of highly stable aluminum mOFs. Chem. Mater. **25**, 17–26 (2013). https://doi.org/10.1021/cm3025445
56. Akiyama, G., Matsuda, R., Kitagawa, S.: Highly porous and stable coordination polymers as water sorption materials. Chem. Lett. **39**, 360–361 (2010). https://doi.org/10.1246/cl.2010.360
57. Jeremias, F., Khutia, A., Henninger, S.K., Janiak, C.: MIL-100(Al, Fe) as water adsorbents for heat transformation purposes—a promising application. J. Mater. Chem. **22**, 10148–10151 (2012). https://doi.org/10.1039/c2jm15615f
58. Wickenheisser, M., Jeremias, F., Henninger, S.K., Janiak, C.: Grafting of hydrophilic ethylene glycols or ethylenediamine on coordinatively unsaturated metal sites in MIL-100(Cr) for improved water adsorption characteristics. Inorg. Chim. Acta. **407**, 145–152 (2013). https://doi.org/10.1016/j.ica.2013.07.024
59. Ehrenmann, J., Henninger, S.K., Janiak, C.: Water adsorption characteristics of MIL-101 for heat-transformation applications of MOFs. Eur. J. Inorg. Chem. **2011**, 471–474 (2011). https://doi.org/10.1002/ejic.201001156

60. Akiyama, G., Matsuda, R., Sato, H., Hori, A., Takata, M., Kitagawa, S.: Effect of functional groups in MIL-101 on water sorption behavior. Microporous Mesoporous Mater. **157**, 89–93 (2012). https://doi.org/10.1016/j.micromeso.2012.01.015
61. Khutia, A., Rammelberg, H.U., Schmidt, T., Henninger, S., Janiak, C.: Water sorption cycle measurements on functionalized MIL-101Cr for heat transformation application. Chem. Mater. **25**, 790–798 (2013). https://doi.org/10.1021/cm304055k
62. Jeremias, F., Lozan, V., Henninger, S.K., Janiak, C.: Programming MOFs for water sorption: amino-functionalized MIL-125 and UiO-66 for heat transformation and heat storage applications. Dalt. Trans. **42**, 15967–15973 (2013). https://doi.org/10.1039/c3dt51471d
63. Shigematsu, A., Yamada, T., Kitagawa, H.: Wide control of proton conductivity in porous coordination polymers. J. Am. Chem. Soc. **133**, 2034–2036 (2011). https://doi.org/10.1021/ja109810w
64. Wade, C.R., Corrales-Sanchez, T., Narayan, T.C., Dincă, M.: Postsynthetic tuning of hydrophilicity in pyrazolate MOFs to modulate water adsorption properties. Energy Environ. Sci. **6**, 2172–2177 (2013). https://doi.org/10.1039/c3ee40876k
65. Liu, J., Wang, Y., Benin, A.I., Jakubczak, P., Willis, R.R., LeVan, M.D.: CO2/H2O adsorption equilibrium and rates on metal-organic frameworks: HKUST-1 and Ni/DOBDC. Langmuir **26**, 14301–14307 (2010). https://doi.org/10.1021/la102359q
66. Schoenecker, P.M., Carson, C.G., Jasuja, H., Flemming, C.J.J., Walton, K.S.: Effect of water adsorption on retention of structure and surface area of metal-organic frameworks. Ind. Eng. Chem. Res. **51**, 6513–6519 (2012). https://doi.org/10.1021/ie202325p
67. Cmarik, G.E., Kim, M., Cohen, S.M., Walton, K.S.: Tuning the adsorption properties of uio-66 via ligand functionalization. Langmuir **28**, 15606–15613 (2012). https://doi.org/10.1021/la3035352
68. Elsayed, E., Al-Dadah, R., Mahmoud, S., Elsayed, A., Anderson, P.A.: Aluminium fumarate and CPO-27(Ni) MOFs: characterization and thermodynamic analysis for adsorption heat pump applications. Appl. Therm. Eng. **99**, 802–812 (2016). https://doi.org/10.1016/j.applthermaleng.2016.01.129
69. Al Dadah, R., Mahmoud, S., Elsayed, E., Youssef, P., Al-Mousawi, F.: Metal-organic framework materials for adsorption heat pumps. Energy **190**, 116356 (2020). https://doi.org/10.1016/j.energy.2019.116356
70. Mohammed, R.H., Rezk, A., Askalany, A., Ali, E.S., Zohir, A.E., Sultan, M., Ghazy, M., Abdelkareem, M.A., Olabi, A.G.: Metal-organic frameworks in cooling and water desalination: synthesis and application. Renew. Sustain. Energy Rev. **149**, 111362 (2021). https://doi.org/10.1016/j.rser.2021.111362
71. Elsayed, A., Elsayed, E., Al-Dadah, R., Mahmoud, S., Elshaer, A., Kaialy, W.: Thermal energy storage using metal–organic framework materials. Appl. Energy. **186**, 509–519 (2017). https://doi.org/10.1016/j.apenergy.2016.03.113
72. Shi, B.: Development of an Mof based adsorption air conditioning system for automotive. http://etheses.bham.ac.uk/id/eprint/6017 (2015)
73. Youssef, P.G., Dakkama, H., Mahmoud, S.M., Al-Dadah, R.K.: Experimental investigation of adsorption water desalination/cooling system using CPO-27Ni MOF. Desalination **404**, 192–199 (2017). https://doi.org/10.1016/j.desal.2016.11.008
74. Dakkama, H.J., Youssef, P.G., Al-Dadah, R.K., Mahmoud, S.: Adsorption ice making and water desalination system using metal organic frameworks/water pair. Energy Convers. Manag. **142**, 53–61 (2017). https://doi.org/10.1016/j.enconman.2017.03.036
75. Rezk, A., Al-Dadah, R., Mahmoud, S., Elsayed, A.: Experimental investigation of metal organic frameworks characteristics for water adsorption chillers. Proc. Inst. Mech. Eng. Part C J. Mech. Eng. Sci. **227**, 992–1005 (2013). https://doi.org/10.1177/0954406212456469
76. Kummer, H., Füldner, G., Henninger, S.K.: Versatile siloxane based adsorbent coatings for fast water adsorption processes in thermally driven chillers and heat pumps. Appl. Therm. Eng. **85**, 1–8 (2015). https://doi.org/10.1016/j.applthermaleng.2015.03.042
77. Cheung, O., Hedin, N.: Zeolites and related sorbents with narrow pores for CO_2 separation from flue gas. RSC Adv. **4**, 14480–14494 (2014). https://doi.org/10.1039/c3ra48052f
78. Elsayed, E., Wang, H., Anderson, P.A., Al-Dadah, R., Mahmoud, S., Navarro, H., Ding, Y., Bowen, J.: Development of MIL-101(Cr)/GrO composites for adsorption heat pump applications. Microporous Mesoporous Mater. **244**, 180–191 (2017). https://doi.org/10.1016/j.micromeso.2017.02.020
79. Jänchen, J., Ackermann, D., Stach, H., Brösicke, W.: Studies of the water adsorption on zeolites and modified mesoporous materials for seasonal storage of solar heat. Sol. Energy. **76**, 339–344 (2004). https://doi.org/10.1016/j.solener.2003.07.036
80. Casey, S.P., Elvins, J., Riffat, S., Robinson, A.: Salt impregnated desiccant matrices for "open" thermochemical energy storage-selection, synthesis and characterisation of candidate materials. Energy Build. **84**, 412–425 (2014). https://doi.org/10.1016/j.enbuild.2014.08.028
81. Mrowiec-Białoń, J., Jarzębski, A.B., Lachowski, A.I., Malinowski, J.J., Aristov, Y.I.: Effective inorganic hybrid adsorbents of water vapor by the sol-gel method. Chem. Mater. **9**, 2486–2490 (1997). https://doi.org/10.1021/cm9703280
82. Wu, H., Wang, S., Zhu, D.: Effects of impregnating variables on dynamic sorption characteristics and storage properties of composite sorbent for solar heat storage. Sol. Energy. **81**, 864–871 (2007). https://doi.org/10.1016/j.solener.2006.11.013
83. Mrowiec-Bialoń, J., Lachowski, A.I., Jarzębski, A.B., Gordeeva, L.G., Aristov, Y.I.: SiO2-LiBr nanocomposite sol-gel adsorbents of water vapor: preparation and properties. J. Colloid Interface Sci. **218**, 500–503 (1999). https://doi.org/10.1006/jcis.1999.6406
84. Gordeeva, L.G., Glaznev, I.S., Malakhov, V.V., Aristov, Y.I.: Influence of calcium chloride interaction with silica surface on phase composition and sorption properties of dispersed salt. Russ. J. Phys. Chem. **77**, 1843–1847 (2003)
85. Aristov, Y.I., Tokarev, M.M., Restuccia, G., Cacciola, G.: Selective water sorbents for multiple applications, 2 $CaCl_2$ confined in micropores of silica gel: sorption properties. React. Kinet. Catal. Lett. **59**, 335–342 (1996). https://doi.org/10.1007/BF02068131
86. Simonova, I.A., Freni, A., Restuccia, G., Aristov, Y.I.: Water sorption on composite "silica modified by calcium nitrate." Microporous Mesoporous Mater. **122**, 223–228 (2009). https://doi.org/10.1016/j.micromeso.2009.02.034
87. Aristov, Y.I., Sapienza, A., Ovoshchnikov, D.S., Freni, A., Restuccia, G.: Reallocation of adsorption and desorption times for optimisation of cooling cycles. Int. J. Refrig. **35**, 525–531 (2012). https://doi.org/10.1016/j.ijrefrig.2010.07.019
88. Tanashev, Y.Y., Krainov, A.V., Aristov, Y.I.: Thermal conductivity of composite sorbents "salt in porous matrix" for heat storage and transformation. Appl. Therm. Eng. **61**, 401–407 (2013). https://doi.org/10.1016/j.applthermaleng.2013.08.022
89. Tokarev, M.M., Aristov, Y.I.: Selective water sorbents for multiple applications, 4 $CaCl_2$ confined in silica gel pores: sorption/desorption kinetics. React. Kinet. Catal. Lett. **62**, 143–150 (1997). https://doi.org/10.1007/BF02475725
90. Gordeeva, L.G., Restuccia, G., Cacciola, G., Aristov, Y.I.: Selective water sorbents for multiple applications, 5 LiBr confined in mesopores of silica gel: sorption properties. React. Kinet. Catal. Lett. **63**, 81–88 (1998). https://doi.org/10.1007/BF02475434
91. Ristić, A., Logar, N.Z.: New composite water sorbents $CaCl_2$-PHTS for low-temperature sorption heat storage:

determination of structural properties. Nanomaterials **9**, 27 (2019). https://doi.org/10.3390/nano9010027
92. Ponomarenko, I.V., Glaznev, I.S., Gubar, A.V., Aristov, Y.I., Kirik, S.D.: Synthesis and water sorption properties of a new composite "$CaCl_2$ confined into SBA-15 pores." Microporous Mesoporous Mater. **129**, 243–250 (2010). https://doi.org/10.1016/j.micromeso.2009.09.023
93. Jabbari-Hichri, A., Bennici, S., Auroux, A.: Effect of aluminum sulfate addition on the thermal storage performance of mesoporous SBA-15 and MCM-41 materials. Sol. Energy Mater. Sol. Cells. **149**, 232–241 (2016). https://doi.org/10.1016/j.solmat.2016.01.033
94. Dong, H., Askalany, A.A., Olkis, C., Zhao, J., Santori, G.: Hydrothermal stability of water sorption ionogels. Energy **189**, 116186 (2019). https://doi.org/10.1016/j.energy.2019.116186
95. Askalany, A., Olkis, C., Bramanti, E., Lapshin, D., Calabrese, L., Proverbio, E., Freni, A., Santori, G.: Silica-supported ionic liquids for heat-powered sorption desalination. ACS Appl. Mater. Interfaces. **11**, 36497–36505 (2019). https://doi.org/10.1021/acsami.9b07602
96. Askalany, A.A., Freni, A., Santori, G.: Supported ionic liquid water sorbent for high throughput desalination and drying. Desalination **452**, 258–264 (2019). https://doi.org/10.1016/j.desal.2018.11.002
97. Gordeeva, L.G., Restuccia, G., Freni, A., Aristov, Y.I.: Water sorption on composites "LiBr in a porous carbon." Fuel Process. Technol. **79**(3), 225–231 (2002)
98. Yu, Q., Zhao, H., Sun, S., Zhao, H., Li, G., Li, M., Wang, Y.: Characterization of $MgCl_2$/AC composite adsorbent and its water vapor adsorption for solar drying system application. Renew. Energy. **138**, 1087–1095 (2019). https://doi.org/10.1016/j.renene.2019.02.024
99. Tso, C.Y., Chao, C.Y.H.: Activated carbon, silica-gel and calcium chloride composite adsorbents for energy efficient solar adsorption cooling and dehumidification systems. Int. J. Refrig. **35**, 1626–1638 (2012). https://doi.org/10.1016/j.ijrefrig.2012.05.007
100. Huang, H., Oike, T., Watanabe, F., Osaka, Y., Kobayashi, N., Hasatani, M.: Development research on composite adsorbents applied in adsorption heat pump. Appl. Therm. Eng. **30**, 1193–1198 (2010). https://doi.org/10.1016/j.applthermaleng.2010.01.036
101. Grekova, A., Gordeeva, L., Aristov, Y.: Composite sorbents "li/Ca halogenides inside multi-wall carbon nano-tubes" for thermal energy storage. Sol. Energy Mater. Sol. Cells. **155**, 176–183 (2016). https://doi.org/10.1016/j.solmat.2016.06.006
102. Grekova, A.D., Gordeeva, L.G., Lu, Z., Wang, R., Aristov, Y.I.: Composite "LiCl/MWCNT" as advanced water sorbent for thermal energy storage: sorption dynamics. Sol. Energy Mater. Sol. Cells. **176**, 273–279 (2018). https://doi.org/10.1016/j.solmat.2017.12.011
103. Brancato, V., Gordeeva, L.G., Grekova, A.D., Sapienza, A., Vasta, S., Frazzica, A., Aristov, Y.I.: Water adsorption equilibrium and dynamics of LICL/MWCNT/PVA composite for adsorptive heat storage. Sol. Energy Mater. Sol. Cells. **193**, 133–140 (2019). https://doi.org/10.1016/j.solmat.2019.01.001
104. Hongois, S., Kuznik, F., Stevens, P., Roux, J.J.: Development and characterisation of a new $MgSO_4$-zeolite composite for long-term thermal energy storage. Sol. Energy Mater. Sol. Cells. **95**, 1831–1837 (2011). https://doi.org/10.1016/j.solmat.2011.01.050
105. Chan, K.C., Chao, C.Y.H., Sze-To, G.N., Hui, K.S.: Performance predictions for a new zeolite 13X/$CaCl_2$ composite adsorbent for adsorption cooling systems. Int. J. Heat Mass Transf. **55**, 3214–3224 (2012). https://doi.org/10.1016/j.ijheatmasstransfer.2012.02.054
106. Oh, H.T., Lim, S.J., Kim, J.H., Lee, C.H.: Adsorption equilibria of water vapor on an alumina/zeolite 13X composite and silica gel. J. Chem. Eng. Data. **62**, 804–811 (2017). https://doi.org/10.1021/acs.jced.6b00850
107. Teo, H.W.B., Chakraborty, A.: Water adsorption on various metal organic framework. IOP Conf. Ser. Mater. Sci. Eng. **272**, 012019 (2017). https://doi.org/10.1088/1757-899X/272/1/012019
108. Yan, J., Yu, Y., Ma, C., Xiao, J., Xia, Q., Li, Y., Li, Z.: Adsorption isotherms and kinetics of water vapor on novel adsorbents MIL-101(Cr)@GO with super-high capacity. Appl. Therm. Eng. **84**, 118–125 (2015). https://doi.org/10.1016/j.applthermaleng.2015.03.040
109. Elsayed, E., Anderson, P., Al-Dadah, R., Mahmoud, S., Elsayed, A.: MIL-101(Cr)/calcium chloride composites for enhanced adsorption cooling and water desalination. J. Solid State Chem. **277**, 123–132 (2019). https://doi.org/10.1016/j.jssc.2019.05.026
110. Liu, Z., Gao, W., Qi, X., Lou, F., Lang, H.: Experimental study on salt–metal organic framework composites for water absorption. Inorg. Chim. Acta. **500**, 119214 (2020). https://doi.org/10.1016/j.ica.2019.119214
111. Sapienza, A., Glaznev, I.S., Santamaria, S., Freni, A., Aristov, Y.I.: Adsorption chilling driven by low temperature heat: new adsorbent and cycle optimization. Appl. Therm. Eng. **32**, 141–146 (2012). https://doi.org/10.1016/j.applthermaleng.2011.09.014
112. Aristov, Y.I., Restuccia, G., Tokarev, M.M., Buerger, H.D.D., Freni, A.: Selective water sorbents for multiple applications. 11 $CaCl_2$ confined to expanded vermiculite. React. Kinet. Catal. Lett. **71**, 377–384 (2000). https://doi.org/10.1023/A:1010351815698
113. Tokarev, M., Gordeeva, L., Romannikov, V., Glaznev, I., Aristov, Y.: New composite sorbent $CaCl_2$ in mesopores for sorption cooling/heating. Int. J. Therm. Sci. **41**, 470–474 (2002). https://doi.org/10.1016/S1290-0729(02)01339-X
114. Liu, H., Nagano, K., Togawa, J.: A composite material made of mesoporous siliceous shale impregnated with lithium chloride for an open sorption thermal energy storage system. Sol. Energy. **111**, 186–200 (2015). https://doi.org/10.1016/j.solener.2014.10.044
115. Liu, H., Nagano, K., Sugiyama, D., Togawa, J., Nakamura, M.: Honeycomb filters made from mesoporous composite material for an open sorption thermal energy storage system to store low-temperature industrial waste heat. Int. J. Heat Mass Transf. **65**, 471–480 (2013). https://doi.org/10.1016/j.ijheatmasstransfer.2013.06.021
116. Nakabayashi, S., Nagano, K., Nakamura, M., Togawa, J., Kurokawa, A.: Improvement of water vapor adsorption ability of natural mesoporous material by impregnating with chloride salts for development of a new desiccant filter. Adsorption **17**, 675–686 (2011). https://doi.org/10.1007/s10450-011-9363-1
117. Alsaman, A.S., Ibrahim, E.M.M., Salem Ahmed, M., Ali, E.S., Farid, A.M., Askalany, A.A.: Experimental investigation of sodium polyacrylate-based innovative adsorbent material for higher desalination and cooling effects. Energy Convers. Manag. **266**, 115818 (2022). https://doi.org/10.1016/j.enconman.2022.115818
118. Thu, K., Ng, K.C., Saha, B.B., Chakraborty, A., Koyama, S.: Operational strategy of adsorption desalination systems. Int. J. Heat Mass Transf. **52**, 1811–1816 (2009). https://doi.org/10.1016/j.ijheatmasstransfer.2008.10.012
119. Wu, J.W., Biggs, M.J., Pendleton, P., Badalyan, A., Hu, E.J.: Experimental implementation and validation of thermodynamic cycles of adsorption-based desalination. Appl. Energy. **98**, 190–197 (2012). https://doi.org/10.1016/j.apenergy.2012.03.022
120. Ng, K.C., Thu, K., Saha, B.B., Chakraborty, A.: Study on a waste heat-driven adsorption cooling cum desalination cycle. Int. J. Refrig. **35**, 685–693 (2012). https://doi.org/10.1016/j.ijrefrig.2011.01.008

121. Mitra, S., Kumar, P., Srinivasan, K., Dutta, P.: Performance evaluation of a two-stage silica gel + water adsorption based cooling-cum-desalination system. Int. J. Refrig. **58**, 186–198 (2015). https://doi.org/10.1016/j.ijrefrig.2015.06.018
122. Gao, W., Li, C., Xu, C., Wang, D., Wu, D.: An experimental investigation of salt-water separation in the vacuum flashing assisted with heat pipes and solid adsorption. Desalination **399**, 116–123 (2016). https://doi.org/10.1016/j.desal.2016.08.016
123. Olkis, C., Brandani, S., Santori, G.: Cycle and performance analysis of a small-scale adsorption heat transformer for desalination and cooling applications. Chem. Eng. J. **378**, 122104 (2019). https://doi.org/10.1016/j.cej.2019.122104
124. Olkis, C., Brandani, S., Santori, G.: Design and experimental study of a small scale adsorption desalinator. Appl. Energy. **253**, 113584 (2019). https://doi.org/10.1016/j.apenergy.2019.113584
125. Olkis, C., Brandani, S., Santori, G.: A small-scale adsorption desalinator. Energy Procedia **158**, 1425–1430 (2019). https://doi.org/10.1016/j.egypro.2019.01.345
126. Olkis, C., Al-Hasni, S., Brandani, S., Vasta, S., Santori, G.: Solar powered adsorption desalination for Northern and Southern Europe. Energy **232**, 120942 (2021). https://doi.org/10.1016/j.energy.2021.120942
127. Elsayed, E., Al-Dadah, R., Mahmoud, S., Anderson, P., Elsayed, A.: Experimental testing of aluminium fumarate MOF for adsorption desalination. Desalination **475**, 114170 (2020). https://doi.org/10.1016/j.desal.2019.114170
128. Zhang, H., Ma, H., Liu, S., Wang, H., Sun, Y., Qi, D.: Investigation on the operating characteristics of a pilot-scale adsorption desalination system. Desalination **473**, 114196 (2020). https://doi.org/10.1016/j.desal.2019.114196
129. Kim, Y.D., Thu, K., Masry, M.E., Ng, K.C.: Water quality assessment of solar-assisted adsorption desalination cycle. Desalination **344**, 144–151 (2014). https://doi.org/10.1016/j.desal.2014.03.021
130. Shahzad, M.W., Thu, K., Kim, Y.D., Ng, K.C.: An experimental investigation on MEDAD hybrid desalination cycle. Appl. Energy. **148**, 273–281 (2015). https://doi.org/10.1016/j.apenergy.2015.03.062
131. Son, H.S., Shahzad, M.W., Ghaffour, N., Ng, K.C.: Pilot studies on synergetic impacts of energy utilization in hybrid desalination system: multi-effect distillation and adsorption cycle (MED-AD). Desalination **477**, 114266 (2020). https://doi.org/10.1016/j.desal.2019.114266
132. Askalany, A., Alsaman, A.S., Ghazy, M., Mohammed, R.H., Al-Dadah, R., Mahmoud, S.: Experimental optimization of the cycle time and switching time of a metal organic framework adsorption desalination cycle. Energy Convers. Manag. **245**, 114558 (2021). https://doi.org/10.1016/j.enconman.2021.114558
133. Ghazy, M., Ibrahim, E.M.M., Mohamed, A.S.A., Askalany, A.A.: Experimental investigation of hybrid photovoltaic solar thermal collector (PV/T)-adsorption desalination system in hot weather conditions. Energy **254**, 124370 (2022). https://doi.org/10.1016/j.energy.2022.124370
134. Albaik, I., Badawy Elsheniti, M., Al-Dadah, R., Mahmoud, S., Solmaz, İ: Numerical and experimental investigation of multiple heat exchanger modules in cooling and desalination adsorption system using metal organic framework. Energy Convers. Manag. **251**, 114934 (2022). https://doi.org/10.1016/j.enconman.2021.114934
135. Saleh, M.M., Elsayed, E., Al-Dadah, R., Mahmoud, S.: Experimental testing of wire finned heat exchanger coated with aluminium fumarate MOF material for adsorption desalination application. Therm. Sci. Eng. Prog. **28**, 101050 (2022). https://doi.org/10.1016/j.tsep.2021.101050